Mon. Not. R. Astron. Soc. **000**, 000–000 (0000) Printed 3 February 2012 (MN LaTeX style file v2.2)

Cores in Infra-Red Dark Clouds (IRDCs) seen in the Hi-GAL survey between l = 300 ° and l = 330 °

L. A. Wilcock[1], D. Ward-Thompson[1], J. M. Kirk[1], D. Stamatellos[1], A. Whitworth[1], D. Elia[2], G. A. Fuller[3], A. DiGiorgio[2], M. J. Griffin[1], S. Molinari[2], P. Martin[4], J. C. Mottram[5], N. Peretto[3,6], M. Pestalozzi[2], E. Schisano[2], R. Plume[7], H. A. Smith[8] & M. A. Thompson[9]

[1]*School of Physics and Astronomy, Cardiff University, Queen's Buildings, Cardiff, CF24 3AA, UK*
[5] *School of Physics, University of Exeter, Stocker Road, Exeter, EX4 4QL, UK*
[3] *Jodrell Bank Centre for Astrophysics, School of Physics and Astronomy, University of Manchester, Manchester, M13 9PL, UK*
[2] *Instituto di Fisica dello Spazio Interplanetario, CNR, via Fosso del Cavaliere, I-00133 Roma, Italy*
[4] *Canadian Institute for Theoretical Astrophysics, University of Toronto, Toronto, Canada, M5S 3H8*
[6] *Laboratoire AIM, CEA/DSM-CNRS-Université Paris Diderot, IFRU/Service d'Astrophysique, C.E. Saclay, Orme des merisiers, 91191 Gif-sur-Yvette, France*
[7] *University of Calgary, Dept Physics-Astronomy, Calgary, AB T2N 1N4, Canada*
[8] *Harvard-Smithsonian Center for Astrophysics, 60 Garden Street, Cambridge, MA, 02138, USA*
[9] *Centre for Astrophysics Research, Science and Technology Research Institute, University of Hertfordshire, AL10 9AB, UK*

3 February 2012

ABSTRACT

We have used data taken as part of the *Herschel* infrared Galactic Plane survey (Hi-GAL) to study 3171 infrared-dark cloud (IRDC) candidates that were identified in the mid-infrared (8 μm) by *Spitzer* (we refer to these as '*Spitzer*-dark' regions). They all lie in the range l=300 – 330° and $|b| \leqslant 1$°. Of these, only 1205 were seen in emission in the far-infrared (250–500 μm) by *Herschel* (we call these '*Herschel*-bright' clouds). It is predicted that a dense cloud will not only be seen in absorption in the mid-infrared, but will also be seen in emission in the far-infrared at the longest *Herschel* wavebands (250–500 μm). If a region is dark at all wavelengths throughout the mid-infrared and far-infrared, then it is most likely to be simply a region of lower background infrared emission (a 'hole in the sky'). Hence, it appears that previous surveys, based on *Spitzer* and other mid-infrared data alone, may have over-estimated the total IRDC population by a factor ~2. This has implications for estimates of the star formation rate in IRDCs in the Galaxy. We studied the 1205 *Herschel*-bright IRDCs at 250 μm, and found that 972 of them had at least one clearly defined 250-μm peak, indicating that they contained one or more dense cores. Of these, 653 (67 per cent) contained an 8-μm point source somewhere within the cloud, 149 (15 per cent) contained a 24-μm point source but no 8-μm source, and 170 (18 per cent) contained no 24-μm or 8-μm point sources. We use these statistics to make inferences about the lifetimes of the various evolutionary stages of IRDCs.

Key words: stars: formation – IRDCs

1 INTRODUCTION

Infrared dark clouds (IRDCs) were initially discovered by the *MSX* (Carey et al. 1998; Egan et al. 1998) and *ISO* (Perault et al. 1996) surveys as dark regions seen against the mid-infrared (MIR) background. The densest IRDCs may eventually form massive stars (e.g. Perault et al. 1996; Kauffmann & Pillai 2010), and are presumed to represent the earliest observable stage of high mass star formation. Some IRDCs contain cores without embedded protostars, which are believed to be the high mass equivalent of low-mass prestellar cores (Rathborne et al. 2006; Chambers et al. 2009).

Observations of IRDCs and their cores have shown them to have low temperatures (T<25 K; e.g. Egan et al. 1998; Teyssier et al. 2002) and high densities ($n_H > 10^5$ cm^{-3}; Egan et al. 1998; Carey et al. 1998, 2000). Kinematic calculations have shown that IRDCs are typically at a galactocentric distance of 6 kpc in the fourth quadrant and 5 kpc in the first quadrant of the Galaxy, matching the location of the Scutum-Centaurus arm (Jackson et al. 2008). IRDCs have masses between a few hundred and several thousand solar masses, while masses of cores within IRDCs tend to lie in the range 10–1000 M$_\odot$ (Rathborne et al. 2006; Swift 2009;

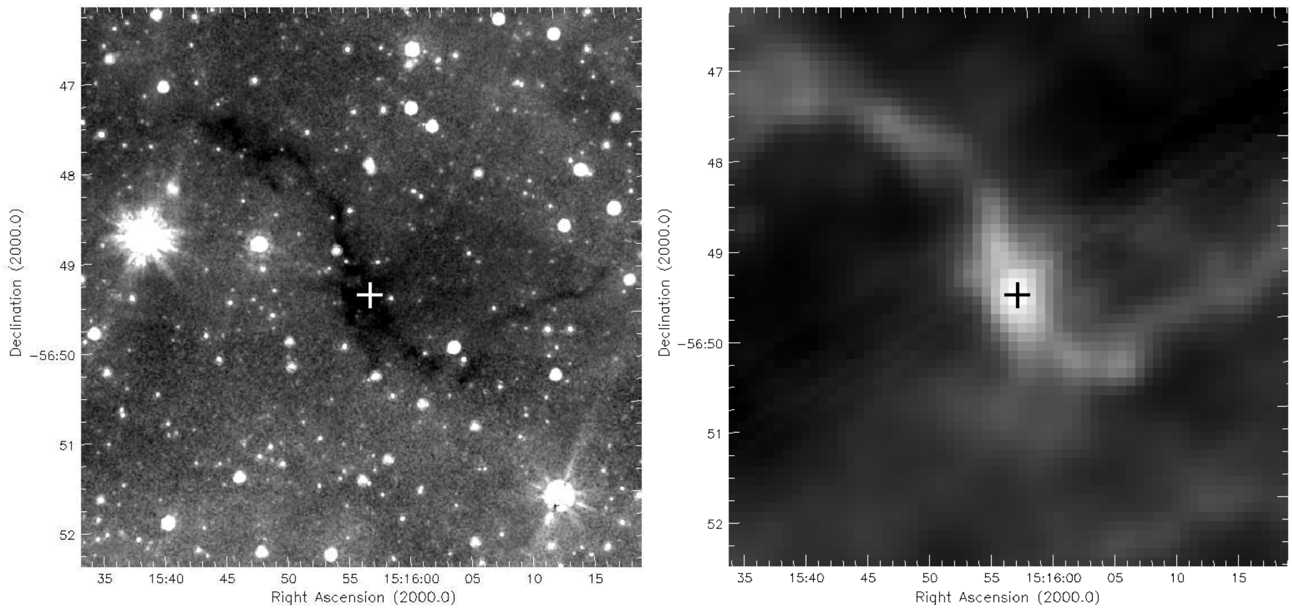

Figure 1. G321.753+0.669. Left panel: 8 μm. Right panel: 250 μm. The position of the candidate IRDC is shown with a cross. This is an example of a *Spitzer*-dark and *Herschel*-bright cloud. Note how the same structure that is seen in absorption (black) in the left panel is seen in emission (white) in the right panel. This is believed to be a genuine IRDC.

Peretto & Fuller 2010; Devine et al. 2011; Wilcock et al. 2011; Zhang et al. 2011).

There are currently two published catalogues of candidate IRDCs, namely Simon et al. (2006) and Peretto & Fuller (2009) – hereafter PF09. The former used 8.3-μm *MSX* data to identify 10931 candidate IRDCs, while the latter used *Spitzer* 8-μm data to find 11303 candidate IRDCs.

Chambers et al. (2009) use a selection of the Simon et al. (2006) IRDCs to propose a hypothetical evolutionary sequence wherein cores evolve from a quiescent to an active phase and finally into a red core. The quiescent cores contain no MIR activity and are likely to be starless, not yet undergoing any star formation. As the core evolves it enters the active phase and begins to show tracers indicating star formation. These tracers include 24-μm emission, maser emission and extended green objects (EGOs; Cyganowski et al. 2008), which are regions of enhanced 4.5-μm emission thought to be shocked H_2 gas (De Buizer & Vacca 2010) and thus charactistic of an outflow, sometimes called ‘green fuzzies’ (Chambers et al. 2009).

A core is said to be in the final, red, stage when it shows PAH emission and is therefore bright at 8 μm. PAH emission is seen in regions with high ultra-violet radiation fields. Hence, red cores may contain hyper-compact or ultra-compact HII regions. Other studies have also used these, or similar, star formation tracers when studying IRDCs (e.g. Jiménez-Serra et al. 2010; Battersby et al. 2011; Devine et al. 2011).

Chambers et al. (2009) had a sample of 190 candidate IRDCs, and they found ∼54 per cent to be quiescent, ∼25 per cent to be active and ∼21 per cent to be red cores. There is some debate over the lifetimes of the different stages of cores in IRDCs. Chambers et al. (2009) use the accretion timescale of high mass star formation and find statistical lifetimes for the quiescent and active phases to be 3.7 and 2.0×10^5 years respectively.

Parsons et al. (2009) had a sample of 69 Simon et al. (2006) IRDCs, and found the ratio to be ∼30 per cent quiescent and ∼70 per cent to have some form of embedded source (either active or red in the Chambers nomenclature). They use a different estimated lifetime for the embedded YSO phase and find a timescale of about an order of magnitude less than Chambers et al. (2009) for the starless, quiescent phase. These lifetime estimates make the assumption that all starless IRDC cores will eventually begin forming high mass stars (Battersby et al. 2010). They should be viewed as no more than order of magnitude estimates at best.

In this paper, we use data from the *Herschel* infrared Galactic Plane Survey (Hi-GAL; Molinari et al. 2010a,b) to observe the IRDCs of PF09 at far-infrared (FIR) wavelengths.

2 OBSERVATIONS

2.1 Herschel

The *Herschel* Space Observatory[1] (Pilbratt et al. 2010) was launched in May 2009, and carries three instruments: the Spectral and Photometric Imaging Receiver (SPIRE, Griffin et al. 2010); the Photodetector Array Camera and Spectrometer (PACS; Poglitsch et al. 2010); and the Heterodyne Instrument for the Far Infrared (HIFI; de Graauw et al. 2010). It is capable of observing in the FIR between 55 and 671 μm. The data used in this paper were taken as part of the *Herschel* infrared Galactic Plane Survey (Hi-GAL), an Open Time Key Project of the *Herschel* Space Observatory (Molinari et al. 2010a,b). Hi-GAL aims to perform a survey of the Galactic Plane using the PACS and SPIRE instruments. The two are used in parallel mode to map the Milky Way Galaxy simultaneously at five wavelengths (70, 160, 250, 350 and 500 μm), with resolutions up to 5″ at 70 μm.

[1] *Herschel* is an ESA space observatory with science instruments provided by European-led Principal Investigator consortia and with participation from NASA.

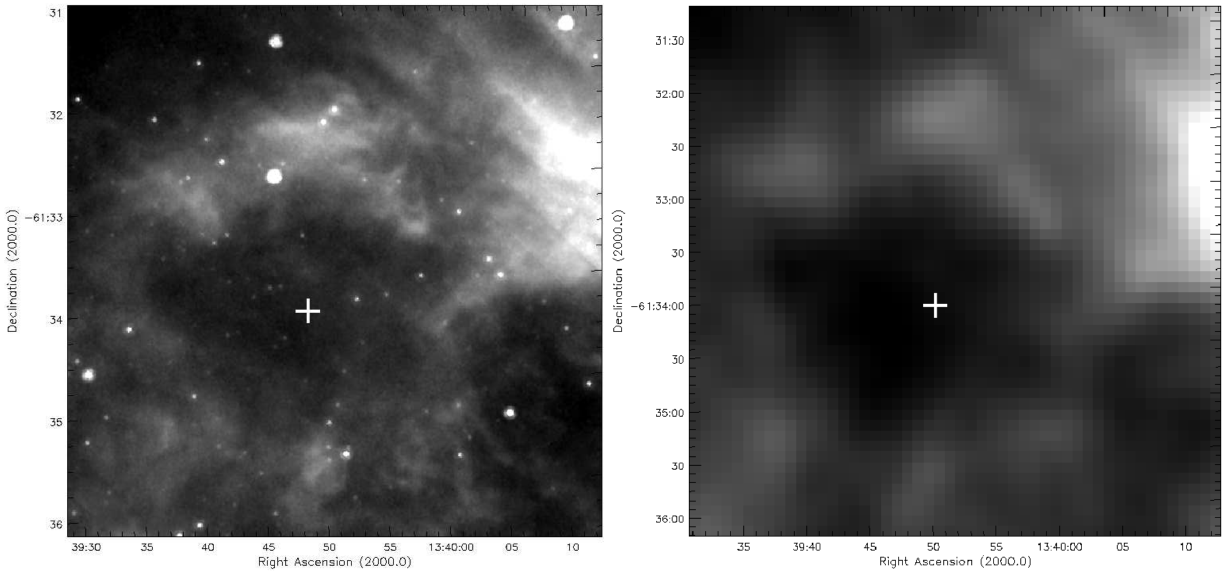

Figure 2. G308.656+0.760. Left panel: 8 μm. Right panel: 250 μm. The position of the candidate IRDC is shown with a cross. This is an example of a candidate IRDC that is *Spitzer*-dark but is not *Herschel*-bright. The same structure that appears dark (black) in the left panel is also dark (black) in the right panel. We refer to such a candidate as *Herschel*-dark. This is not believed to be a genuine IRDC.

PACS data reduction at 70 and 160 μm was performed using the *Herschel* Interactive Pipeline Environment (HIPE; Ott 2010), with some additions described by Poglitsch et al. (2010). The standard deglitching and crosstalk correction were not used and custom procedures were written for drift removal (Traficante et al. 2011). SPIRE data processing at 250, 350 and 500 μm used the standard processing methods (Griffin et al. 2010), with both standard deglitching and drift removal. In all cases, the ROMAGAL Generalised Least Squares algorithm (Traficante et al. 2011) was used to produce the final maps. A more detailed discussion of the data reduction process is given by Traficante et al. (2011).

2.2 Spitzer

The *Spitzer* Space Telescope[2] (Werner et al. 2004) was launched in August 2003, and carried three instruments: the Multiband Infrared Photometer for *Spitzer* (MIPS; Rieke et al. 2004); the Infrared Array Camera (IRAC; Fazio et al. 2004); and the Infrared Spectograph (IRS; Houck et al. 2004). These instruments are capable of observing in a number of wavebands ranging between 3.6 and 160 μm. As part of its legacy science programme, *Spitzer* performed two surveys of the Galactic Plane. These were the MIPS Galactic Plane Survey (MIPSGAL; Carey et al. 2009) and the Galactic Legacy Infrared Mid-Plane Survey Extraordinaire (GLIMPSE; Benjamin et al. 2003). Here, we use the mosaics made available by the *Spitzer* Science Centre to create 8- and 24-μm maps of the region encompassing $300^\circ \leqslant l \leqslant 330^\circ$, and $|b| \leqslant 1^\circ$.

[2] *Spitzer* was operated by the Jet Propulsion Laboratory at the California Institute of Technology under a contract with NASA.

3 RESULTS

3.1 Classifying IRDCs

The PF09 catalogue used *Spitzer* 8-μm data to find 11303 candidate IRDCs in the regions $10^\circ < l < 65^\circ$ and $295^\circ < l < 350^\circ$ with $|b| < 1^\circ$. They identified candidate IRDCs as connected structures with an apparent mean 8-μm opacity greater than 0.35 and an apparent peak above 0.7. This would correspond to a molecular hydrogen column density (N_{H_2}) detection threshold of a mean of $\sim 10^{22}$, and a peak of $\sim 2 \times 10^{22}$ cm^{-2}, respectively. Each candidate IRDC had to be at least 4″ in diameter. We refer to these regions as '*Spitzer*-dark' regions. To find the embedded cores (which PF09 termed fragments), they used apparent opacity contours with a step of 0.35. The number of local peaks between each consecutive level was then the number of fragments extracted.

We present data here on the region from l = 300° to l = 330° with $|b| < 1^\circ$. This region was chosen as it was the first large contiguous area to be covered in the Hi-GAL survey. It had also been observed in both the GLIMPSE and MIPSGAL surveys and was included in the PF09 survey. The region was therefore used to search for IRDCs and their cores. The PF09 catalogue contained 3171 *Spitzer*-dark candidate IRDCs in this region. Identifying IRDCs in the MIR alone can cause problems. IRDCs appear as dark regions against the bright MIR background. However, there is no way in the MIR of distinguishing between an area of low emission caused by absorption by an IRDC and an area of low emission caused by a local dip in the MIR background, sometimes referred to as a 'hole in the sky' (Stanke et al. 2010). One way of identifying genuinely dense, cold regions is to look for emission in the far-infrared (FIR), where cold dust should emit strongly. We label such regions as '*Herschel*-bright' (referring only to the longer wavelength *Herschel* data).

We studied each of the 3171 objects within our search area in the PF09 catalogue, using *Spitzer* data at 8 and 24 μm, and *Herschel* data at 70, 160, 250, 350 and 500 μm, to determine which of the objects were real IRDCs and which were just local dips in the MIR emission. Some examples are shown in Figures 1–4. Each

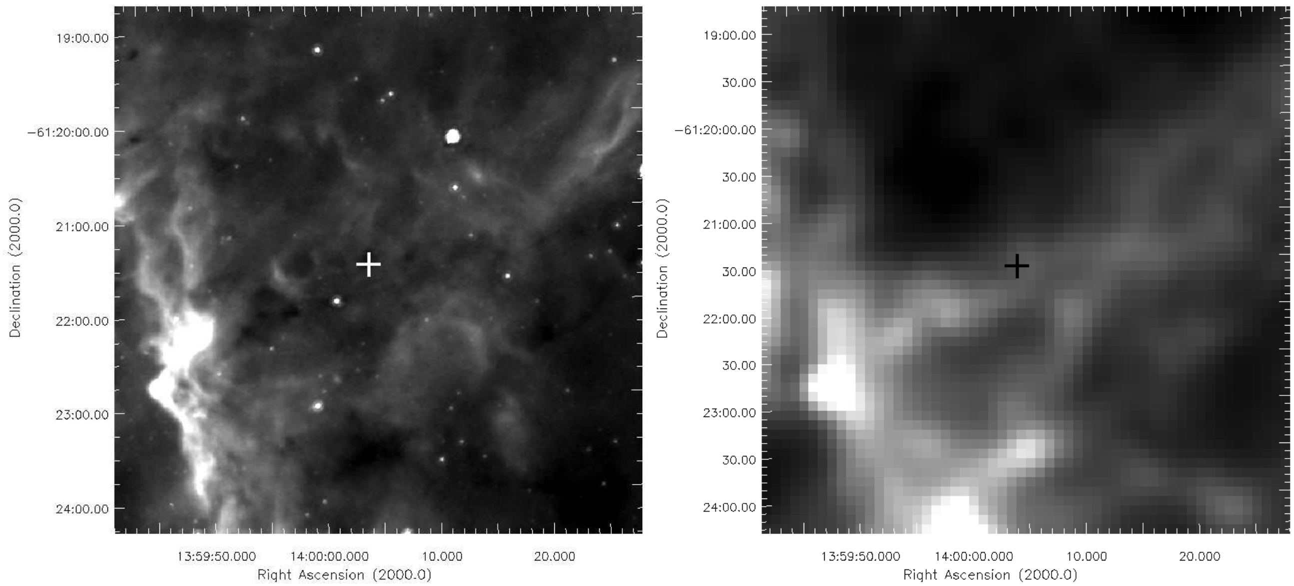

Figure 3. G311.061+0.425. Left panel: 8 μm. Right panel: 250 μm. The position of the IRDC is marked with a cross. This is an example of a genuine *Spitzer*-dark, *Herschel*-bright IRDC. However, it does not appear to contain any dense cores. Only diffuse and filamentary emission can be seen at 250 μm.

candidate IRDC was viewed in a similar fashion to Figures 1–4 but at all six wavelengths. Any object seen in absorption at 8 μm and seen simultaneously in emission at 250, 350 and 500 μm was classed as both *Spitzer*-dark and *Herschel*-bright, and was classified as a genuine IRDC. An example of a *Spitzer*-dark and *Herschel*-bright IRDC can be seen in Figure 1. The full list of *Herschel*-bright IRDCs is given in Appendix A.

At 70 μm a cloud may be expected to be seen in absorption, but less strongly than at 8 μm. Furthermore, the noise in the 70-μm data sometimes tended to make it unclear whether the core was in emission or absorption at 70 μm. Likewise, a source's appearance at 160 μm depends heavily on the temperature of the cloud. For these reasons, the 70- and 160-μm wavelengths were not used in the initial classification process, and were only used when the other wavelengths left some ambiguity about a source's status.

Sensitivity limits on *Herschel* mean that smaller, less dense IRDCs are not likely to show enough emission to be classified as *Herschel*-bright. We estimate that any IRDC with a major axis less than 26$''$and a peak column density less than $4{\times}10^{22}$ cm^{-2} will not be visible in emission at 250, 350 or 500 μm if it is situated in a region with a background greater than 1300 MJy/sr at 250 μm. This accounts for approximately 20 per cent of the PF09 objects. As it cannot be stated whether these objects are emitting in the FIR or not, their true status is unknown and they remain candidate IRDCs. Further details can be found in Appendix B.

In total, of the original 3171 objects in the PF09 catalogue in our search area, we found only 1205 of them to be genuine IRDCs under our simultaneous *Spitzer*-dark and *Herschel*-bright definition. These objects are listed in Table A1 of Apeendix A. We note that *Herschel* is insensitive to ~20 per cent of the candidates, see Appendix B.

This method relies upon human interpretation of the data. To estimate the error-bars introduced by this method a second person observed all the candidates in a circular region with a radius of 0.5°. They classified each candidate as *Herschel*-bright or *Herschel*-dark as before. Of the 107 candidate IRDCs in this region, only three were classified differently by the second person.

This implies that all previous catalogues of IRDCs, based solely on MIR data, may have over-estimated the total number of IRDCs in the Galaxy. In this region the number has been over-estimated by up to a factor of ~1.7–2.6. Similar factors might be expected elsewhere. Jackson et al. (2008) carried out a 'reliability' test on the IRDC catalogue of Simon et al. (2006), and found values ranging from ~50 per cent to ~100 per cent for the fraction of genuine IRDCs in the catalogue, depending on the contrast level in the MIR. In other words, they found up to a factor of ~2 over-estimate in the number of genuine IRDCs – consistent with our results.

The discovery that only 1205 of the candidate IRDCs, in a catalogue based on MIR data, turn out to be *Herschel*-bright (see upper part of Table 1) has ramifications for all such catalogues based on MIR data alone. The total number of candidate IRDCs in the catalogues of Simon et al. (2006) and PF09 is ~11000 in each. If our observed ratio is consistent throughout these catalogues, then the total number of genuine IRDCs in each may be as low as ~4000–6000 (c.f. Jackson et al. 2008). This has consequences for calculations of the total number of IRDCs in the Galaxy.

3.2 Cores within IRDCs

Each cloud was examined at 250 μm. Some IRDCs were seen to have relatively simple structures, while others had more complex structures. The 250-μm band was chosen as this had the best resolution of the three wavelengths where the IRDCs were predicted to be seen in emission. Each cloud was examined for evidence that one or more dense cores had formed within the cloud.

A gaussian profile was fitted towards the peak of the intensity map of each core at 250 μm. Our criteria for classification as *Herschel*-bright specified that a candidate IRDC had to be seen in emission at 250, 350 and 500 μm. The emission from each of our *Herschel*-bright IRDCs was therefore much greater than its surrounding background. As such, no background subtraction was needed when fitting the gaussian profiles.

The gaussian fitted at 250 μm was used to determine the full-width at half-maximum (FWHM) of each core. Some IRDCs could

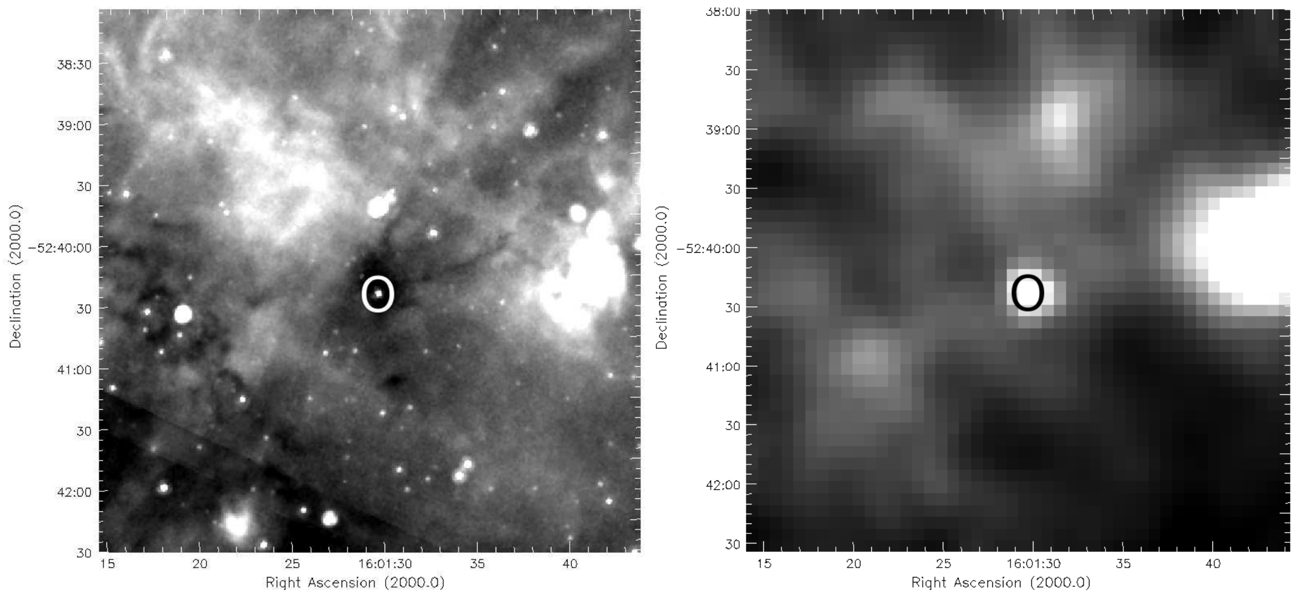

Figure 4. G329.494+0.106. Left panel: 8 μm. Right panel: 250 μm. This is an example of a genuine *Spitzer*-dark and *Herschel*-bright IRDC, which contains an 8-μm point source. The point source is circled in both panels.

be fitted with more than one gaussian, indicating the presence of more than one dense core. A total of 972 IRDCs fell into the category of having one or more dense cores within them.

In the case of 215 IRDCs, cloud emission was seen in the FIR at 250 μm, but there was no discernible 250-μm peak. These IRDCs were deemed not to have any dense cores within them. For 18 IRDCs the data were found to be excessively 'stripy' at 250 μm, resulting in no gaussian being able to be fitted. These were discarded. These 233 objects, to which no gaussian could be fitted, were omitted from further consideration. This left us with a 'clean' sample of 972 IRDCs that contain one or more dense cores, on which we concentrate for the remainder of the paper.

3.3 Protostars within IRDC cores

The 972 IRDCs containing one or more dense cores were studied closely in the 8-μm data for evidence of an 8-μm point source. The presence or lack of an 8-μm point source within a core is most likely to be indicative of the presence or absence of an embedded protostar. Hence, this is an indication of the evolutionary status of the core. More evolved cores, namely those already undergoing star formation, are more likely to have an 8-μm point source within them.

Every core in all of the 972 IRDCs was searched for an embedded 8-μm point source. An 8-μm point source was defined as a compact, roughly circular source with an 8-μm peak of greater than 3σ, where σ is the noise level of the data and was defined as the standard deviation in flux towards the edge of each region. The peak of the point source had to be within a radius from the centre of the core (defined at 250 μm) equal to the FWHM of the core at 250 μm. It should be noted that, as no distance information is available for the majority of these IRDCs, it is possible that the 8 μm point sources noted here are, in some cases, not associated with the IRDC itself but are instead foreground stars contaminating the field of view (see also Lumsden et al. 2002). 653 out of 972 IRDCs (67 per cent) were found to have at least one 8-μm point source embedded in one or more of their constituent cores. This left 319 IRDCs with no 8-μm point source.

These 319 IRDCs without 8-μm point sources were searched for a 24-μm point source. The search was carried out using the same criteria as when looking for an 8-μm point source. Of the 319 IRDCs, 149 were found to have one or more 24-μm point sources.

In summary, we found a total of 972 IRDCs that contained one or more discernable cores at 250 μm. Of these, 653 have an 8-μm point source. Of the IRDCs with no 8-μm point source, a further 149 have a 24-μm point source. We designate the remaining 170 as starless IRDCs. These objects could be the high-mass equivalents of low-mass starless cores. The total number of IRDCs in each category is summarised in Table 1.

4 DISCUSSION

4.1 Statistics

The relative numbers of IRDCs with no embedded MIR point sources, compared to those with 8- and 24-μm point sources (see lower part of Table 1), can be used for comparison with previous findings. Chambers et al. (2009) labelled IRDCs with no embedded MIR point sources as quiescent, those with a 24-μm point source as active, and those with an 8-μm point source as red cores. They had a sample of 190 candidate IRDCs, and found ~21 per cent to be red, ~25 per cent to be active and ~54 per cent to be quiescent. These percentages can be compared to the last three lines in Table 1.

It can be seen that there is a much larger fraction of quiescent IRDCs in the Chambers sample than in ours. This could be due to the effect of some fraction of their initial sample of candidate IRDCs not being genuine, as they had no FIR data. Interestingly, though, because they see 46 per cent of their candidate IRDCs having other star formation tracers, then only a maximum of 54 per cent (±5 per cent) of their candidate IRDCs could be false, compared to up to 62 per cent (±1 per cent) in our full sample (although note that some of their associations could be chance alignments). However,

Table 1. IRDC statistics. The upper part of the Table lists the number and percentage of candidates in the PF09 catalogue that were found to be *Herschel*-bright. The lower part of the Table refers to the sample of 972 IRDCs that contained one or more dense cores at 250 μm, and lists those with embedded 8-μm sources, those without 8-μm sources that contain 24-μm sources, and those with neither 8-μm nor 24-μm sources.

Source Type	Equivalent Class of Chambers et al. (2009)	Number of IRDCs	Percentage
PF09 sample		3171	100
Herschel-bright		1205	38
IRDCs with cores		972	100
IRDCs with 8-μm source	Red Core	653	67
IRDCs with 24-μm source only	Active Core	149	15
No 8- or 24-μm source	Quiescent Core	170	18

Chambers et al. (2009) have a much smaller sample of cores. Additionally, Chambers et al. (2009) use the Simon et al. (2006) catalogue of candidate IRDCs. The Simon et al. (2006) catalogue was based on *MSX* data and used different criteria to PF09 when finding candidate IRDCs. This makes a detailed comparison between this work and that of Chambers et al. (2009) difficult. The errors quoted in brackets here are simply the poisson ($\sqrt{n}$) errors, and there may also be systematic effects at work. Hence, these two numbers are roughly consistent.

Parsons et al. (2009) cross-matched the candidate IRDCs of Simon et al. (2006) with SCUBA 850-μm emission, and found that 25 per cent of the candidate IRDCs were not seen in emission at 850 μm. Of those that were detected by SCUBA, which also appeared in the GLIMPSE survey, they found that 70 per cent had embedded 24-μm point sources, and 30 per cent did not. They made no distinction between those 24-μm sources that also had 8-μm point sources and those that did not. Hence their 30 per cent needs to be compared to the last line in Table 1 (18 per cent), and their 70 per cent should be compared to the sum of the two lines above that in Table 1 (82 per cent). Given the very different sizes of the samples (the simple poisson $\sqrt{n}$ errors on their numbers are $\sim \pm 10$ per cent), these are also consistent with the percentages we find.

4.2 Relative lifetimes

A simple evolutionary picture for a core within an IRDC is given by Chambers et al. (2009). This entails a quiescent, starless core evolving first into a core with an embedded 24-μm point source. This phase could be equated theoretically with the main accretion phase for massive protostar formation. Subsequently the core would evolve into a core with an embedded 8-μm point source, indicating the beginnings of an HII region starting to form. If each starless IRDC core evolves into a corresponding star-forming core with one or more embedded 24-μm point sources, and each of these evolves into a core with the same number of embedded 8-μm point sources, then we can equate the above statistics with theoretical lifetimes, and produce statistical lifetimes for each of the stages in Table 1.

One clear result that then comes from Table 1 is that only about one-fifth of IRDC cores do not contain embedded point sources. If this corresponds to the 'starless' phase of IRDCs, then we would conclude that a typical IRDC core only spends around one-fifth of its lifetime without any seed of a protostar within it. Chambers et al. (2009) assume that the accretion timescale of high mass star formation is equivalent to the amount of time that an IRDC core will exist in the active phase (i.e. has a 24-μm point source, but no 8-μm point source). We can use a canonical value for the accretion timescale of $\sim 2\times10^5$ years (Zinnecker & Yorke 2007) as the lifetime for the active phase.

Hence we would calculate, from the similarity of the percentages in the last two lines of Table 1, that the lifetime of the quiescent, or starless, phase of IRDCs is also $\sim 2\times10^5$ years. Similarly, the lifetime of the phase with an embedded 8-μm source (the red stage in Chambers' nomenclature) would then be $\sim 6\times10^5$ years and the entire IRDC lifetime (after core formation) would be $\sim 10^6$ years. Chambers et al. (2009) find $\sim 4\times10^5$ years for the quiescent phase, also by assuming 2×10^5 years for the active phase.

The 8-μm emission is believed to arise from very hot, very small grains, known as polycyclic aromatic hydrocarbons (PAHs; Chambers et al. 2009). A typical PAH is so small that a single high-energy photon can interact with a PAH and raise its temperature to a few hundred degrees for a short period of time, before it cools again by re-emitting a photon in the MIR. Such high-energy photons are presumed to ionise the surrounding material and create hyper-compact and ultra-compact HII (HCHII and UCHII) regions. Hence the phase where an IRDC contains an embedded 8-μm point source should roughly correlate with the combined HCHII and UCHII phases. The UCHII lifetime is not well known, although recent estimates put it at several $\times 10^5$ years (e.g. Kaper et al. 2011), consistent with our estimate. Similarly, McKee & Tan (2002) look at stars in typical regions of high mass star formation and find timescales of a few $\times10^5$ years for the combined HCHII and UCHII phases. This is also consistent with our estimated lifetime of the phase in which an IRDC has an embedded 8-μm point source.

5 CONCLUSIONS

3171 candidate IRDCs were catalogued from their MIR absorption in *Spitzer* data (*Spitzer*-dark regions). We found 1205 which are *Herschel*-bright. The other objects may be simply minima in the IR background. This suggests that IRDC searches based solely on MIR data may over-estimate the total number of IRDCs in the Galaxy by up to a factor of ∼2.

972 of the 1205 *Herschel*-bright IRDCs have one or more discernible peaks at 250 μm, indicating the formation of dense cores within these IRDCs. The *Spitzer* data were then examined to see whether the IRDCs with cores contained either an 8- or a 24-μm point source. 653 are seen to harbour one or more 8-μm point sources, and of the remainder, a further 149 contained one or more 24-μm point sources.

We equated the presence of a 24-μm point source to the typical accretion timescale for high-mass stars of $\sim 2\times10^5$ years and hence derived a timescale for the starless IRDC core phase also of $\sim 2\times10^5$ years. We equated the presence of an 8-μm point source to the combined HCHII and UCHII phase, and derived a timescale of $\sim 6\times10^5$ years for this stage. A total lifetime for IRDCs with dense cores of $\sim 10^6$ years was thus derived.

ACKNOWLEDGEMENTS

LAW acknowledges STFC studentship funding. SPIRE was developed by a consortium of institutes led by Cardiff University (UK) and including Univ. Lethbridge (Canada); NAOC (China); CEA, LAM (France); IFSI, Univ. Padua (Italy); IAC (Spain); Stockholm Observatory (Sweden); Imperial College London, RAL, UCL-MSSL, UKATC, Univ. Sussex (UK); and Caltech, JPL, NHSC, Univ. Colorado (USA). This development was supported by national funding agencies: CSA (Canada); NAOC (China); CEA, CNES, CNRS (France); ASI (Italy); MCINN (Spain); SNSB (Sweden); STFC (UK); and NASA (USA). PACS was developed by a consortium of institutes led by MPE (Germany) and including UVIE (Austria); KU Leuven, CSL, IMEC (Belgium); CEA, LAM (France); MPIA (Germany); INAF-IFSI/OAA/OAP/OAT, LENS, SISSA (Italy); IAC (Spain). This development was supported by the funding agencies BMVIT (Austria), ESA-PRODEX (Belgium), CEA/CNES (France), DLR (Germany), ASI/INAF (Italy), and CICYT/MCYT (Spain). HIPE is a joint development by the *Herschel* Science Ground Segment Consortium, consisting of ESA, the NASA *Herschel* Science Center, and the HIFI, PACS and SPIRE consortia. This work is also based, in part, on observations made with the *Spitzer* Space Telescope, which is operated by the Jet Propulsion Laboratory, California Institute of Technology under a contract with NASA.

REFERENCES

Battersby C., Bally J., Ginsburg A., et al., 2011. ArXiv e-prints. 1101.4654
Battersby C., Bally J., Jackson J.M., Ginsburg A., Shirley Y.L., Schlingman W., Glenn J., 2010. ApJ, 721, 222
Benjamin R., Churchwell E., Babler B.L., et al., 2003. PASP, 113, 953
Black J.H., 1994. In The First Symposium on the Infrared Cirrus and Diffuse Interstellar Clouds. vol. 58 of ASP Conference Series, p. 355
Carey S., Clark F., Egan M., Price S., Shipman R., Kuchar T., 1998. ApJ, 508, 721
Carey S., Feldman P., Redman R., Egan M., MacLeod J., Price S., 2000. ApJ, 543, 157
Carey S., Noriega Crespo A., Mizuno D.R., et al., 2009. PASP, 121, 76
Chambers E., Jackson M., Rathborne J., Simon R., 2009. ApJS, 181, 360
Cyganowski C.J., Whitney B.A., Holden E., et al., 2008. AJ, 136, 2391. 0810.0530
De Buizer J.M., Vacca W., 2010. A&A, 140, 196
de Graauw T., Helmich F.P., Phillips T.G., et al., 2010. AAP, 518, L6+
Devine K.E., Chandler C.J., Brogan C., Churchwell E., Indebetouw R., Shirley Y., Borg K.J., 2011. ApJ, 733, 44
Egan M., Shipman R., Price S., Carey S., Clark F., Cohen M., 1998. ApJ, 494, 199
Fazio G., Hora J., Allen L., et al., 2004. ApJS, 154, 10
Griffin M.J., Abergel A., Ade P., et al., 2010. A&A, 518, L3
Houck J.R., Roellig T.L., van Cleve J., et al., 2004. APJS, 154, 18
Jackson J., Finn S., Rathborne J., Chambers E., Simon R., 2008. ApJ, 680, 349
Jiménez-Serra I., Caselli P., Tan J.C., Hernandez A.K., Fontani F., Butler M.J., van Loo S., 2010. MNRAS, 406, 187
Kaper L., Ellerbroek L.E., Ochsendorf B.B., Caballero Pouroutidou R.N., 2011. Astronomische Nachrichten, 332, 232
Kauffmann J., Pillai T., 2010. ApJL, 723, L7
Lenfestey C., Peretto N., Fuller G., et al., 2012. in prep
Lumsden S.L., Hoare M.G., Oudmaijer R.D., Richards D., 2002. MNRAS, 336, 621. arXiv:astro-ph/0206391
McKee C.F., Tan J.C., 2002. Nature, 416, 59. arXiv:astro-ph/0203071
Molinari S., Swinyard B., Bally J., et al., 2010a. A&A, 518, L100
Molinari S., Swinyard B., Bally J., et al., 2010b. PASP, 122, 314
Ossenkopf V., Henning T., 1994. A&A, 291, 943
Ott S., 2010. In Mizumoto Y., Morita K.I., Ohishi M., eds., Astronomical Data Analysis Software and Systems XIX. ASP Conference Series
Parsons H., Thompson M.A., Chrysostomou A., 2009. MNRAS, 399, 1506
Perault M., Omont A., Simon G., et al., 1996. A&A, 315, 165
Peretto N., Fuller G.A., 2009. A&A, 505, 405. PF09
Peretto N., Fuller G.A., 2010. ApJ, 723, 555
Pilbratt G.L., Riedinger J.R., Passvogel T., et al., 2010. A&A, 518, L1
Poglitsch A., Waelkens C., Geis N., et al., 2010. A&A, 518, L2
Rathborne J.M., Jackson J.M., Simon R., 2006. ApJ, 641, 389
Rieke G., Young E., Engelbracht C., et al., 2004. ApJS, 154, 25
Simon R., Jackson J., Rathborne J., Chambers E., 2006. ApJ, 639, 227
Stamatellos D., Griffin M., Kirk J., Molinari S andSibthorpe B., Ward Thompson D., Whitworth A., Wilcock L., 2010. MNRAS, 1204
Stamatellos D., Whitworth A., 2003. A&A, 407, 941
Stamatellos D., Whitworth A., 2005. A&A, 439, 159
Stanke T., Stutz A.M., Tobin J.J., et al., 2010. A&A, 518, L94+
Swift J.J., 2009. ApJ, 705, 1456
Teyssier D., Hennebelle P., Perault M., 2002. A&A, 382, 624
Traficante A., Calzoletti L., Veneziani M., et al., 2011. MNRAS, pp. 1373–+
Werner M., Roellig T., Low F., et al., 2004. ApJS, 154, 25
Wilcock L.A., Kirk J.M., Stamatellos D., et al., 2011. A&A, 526, A159+
Wilcock L.A., Kirk J.M., Stamatellos D., et al., 2012. in prep
Zhang S.B., Yang J., Xu Y., Pandian J.D., Menten K.M., Henkel C., 2011. ApJS, 193, 10
Zinnecker H., Yorke H.W., 2007. ARAA, 45, 481

APPENDIX A: LIST OF HERSCHEL-BRIGHT IRDCS

Table A1: The 1,205 IRDCs which were found to be *Herschel*-bright. Column 1 states the IRDC name as it appears in PF09. Columns 2 and 3 are the position of the IRDC. Columns 4 and 5 give details on whether the object contains a MIR source. Column 6 gives additional information about the cloud, including whether it contains a visible core and whether it is isolated at 160 and 500 μm.

IRDC Name	Right Ascension 2000.0 (°)	Declination 2000.0 (°)	8 μm source?	24 μm source?	Additional comments
300.345−0.357	187.13	−63.11	Yes		
300.356−0.358	187.16	−63.12	Yes		
300.596+0.098	187.77	−62.68	Yes		
300.743+0.036	188.08	−62.75	Yes		
300.746+0.550	188.16	−62.24	Yes		
301.131−0.274	188.88	−63.09	Yes		
301.206−0.193	189.06	−63.01	No	No	Confused at 500 μm
301.283−0.242	189.22	−63.07	Yes		
301.423−0.116	189.54	−62.95	Yes		
301.504−0.464	189.68	−63.30	Yes		
301.512−0.350	189.71	−63.19	No	No	Confused at 500 μm
301.519−0.467	189.71	−63.30	Yes		
301.550−0.121	189.82	−62.96	Yes		
301.558−0.380	189.81	−63.22	Yes		
301.595−0.107	189.92	−62.95	Yes		
301.605−0.118	189.94	−62.96	Yes		
301.659−0.367	190.04	−63.21	Yes		
301.659+0.245	190.09	−62.60	No	No	Confused at 500 μm
301.671−0.201	190.08	−63.05	Yes		
301.689−0.414	190.10	−63.26	Yes		
301.785+0.145	190.36	−62.70	Yes		
301.861+0.694	190.57	−62.16	No	Yes	
301.876+0.589	190.59	−62.26	Yes		
302.097+0.233	191.04	−62.63	Yes		
302.172+0.258	191.21	−62.60	Yes		
302.458−0.783	191.79	−63.65	Yes		
302.543+0.000	192.01	−62.87	Yes		
302.593+0.122	192.12	−62.75	Yes		
302.688+0.084	192.33	−62.79	Yes		
302.764−0.082	192.49	−62.95	No	No	Confused at 500 μm
302.813−0.034	192.60	−62.91	Yes		
302.844+0.235	192.67	−62.64	Yes		
302.847−0.049	192.67	−62.92	No	No	Confused at 500 μm
302.883−0.431	192.75	−63.30	Yes		
302.939−0.445	192.88	−63.32	Yes		
303.043−0.449	193.11	−63.32	No	Yes	
303.044−0.434	193.11	−63.31	Yes		
303.049+0.113	193.12	−62.76	Yes		
303.059−0.450	193.14	−63.32	Yes		
303.359+0.418	193.78	−62.45	Yes		
304.013+0.485	195.19	−62.37	No	No	Confused at 500 μm
304.115+0.279	195.43	−62.57	Yes		
304.132−0.384	195.53	−63.23	Yes		
304.526−0.037	196.36	−62.87	Yes		
304.584+0.333	196.44	−62.49	No	Yes	
304.601+0.353	196.47	−62.47	No	No	Confused at 500 μm
304.723+0.266	196.75	−62.55	Yes		
304.795+0.202	196.91	−62.61	No	Yes	
304.812+0.222	196.95	−62.59	Yes		
304.816+0.431	196.93	−62.38	Yes		
304.823+0.324	196.96	−62.49	Yes		

continued on next page

IRDC Name	Right Ascension 2000.0 (°)	Declination 2000.0 (°)	8 μm source?	24 μm source?	Additional comments
304.831+0.336	196.97	−62.47	Yes		
304.836+0.578	196.95	−62.23	No	Yes	
304.856+0.270	197.04	−62.54	Yes		
305.022+0.325	197.39	−62.47			No distinct core
305.045+0.446	197.42	−62.35	Yes		
305.049+0.561	197.41	−62.24	Yes		
305.059−0.170	197.54	−62.96	Yes		
305.079+0.660	197.46	−62.13	Yes		
305.083+0.258	197.53	−62.54	No	Yes	
305.085−0.166	197.60	−62.96			No distinct core
305.086+0.548	197.49	−62.25	Yes		
305.103+0.582	197.52	−62.21	Yes		
305.131−0.027	197.68	−62.82	No	Yes	
305.134+0.067	197.67	−62.72	Yes		
305.162+0.224	197.70	−62.56	No	Yes	
305.162+0.554	197.65	−62.23	Yes		
305.183+0.464	197.71	−62.32	No	No	Confused at 500 μm
305.183+0.475	197.71	−62.31	Yes		
305.200+0.001	197.82	−62.78	Yes		
305.209+0.205	197.81	−62.58	Yes		
305.228+0.270	197.84	−62.51	Yes		
305.307−0.259	198.10	−63.03			No distinct core
305.339−0.254	198.17	−63.03	No	No	Confused at 500 μm
305.376+0.461	198.13	−62.31	Yes		
305.412+0.355	198.22	−62.41	Yes		
305.425+0.436	198.24	−62.33	No	Yes	
305.433−0.262	198.38	−63.03	No	Yes	
305.440+0.109	198.33	−62.66	Yes		
305.498+0.180	198.44	−62.58	Yes		
305.504+0.168	198.46	−62.59	Yes		
305.523+0.402	198.45	−62.36	Yes		
305.540+0.434	198.48	−62.32	Yes		
305.547−0.054	198.59	−62.81	Yes		
305.575−0.342	198.71	−63.09	Yes		
305.590+0.333	198.61	−62.42	Yes		
305.595+0.392	198.61	−62.36	Yes		
305.595+0.421	198.60	−62.33	Yes		
305.633−0.043	198.78	−62.79	Yes		
305.651−0.008	198.81	−62.75	No	Yes	
305.688−0.025	198.89	−62.77	Yes		
305.689+0.423	198.80	−62.32			No distinct core
305.696−0.147	198.94	−62.89	Yes		
305.706+0.026	198.92	−62.71	Yes		
305.741+0.163	198.97	−62.57	Yes		
305.798−0.097A	199.15	−62.83	No	No	
305.798−0.097B	199.15	−62.83	Yes		
305.801+0.120	199.11	−62.61	No	Yes	
305.818−0.073	199.18	−62.80	No	Yes	
305.866−0.148	199.31	−62.87	Yes		
305.898−0.029A	199.35	−62.75	Yes		
305.898−0.029B	199.35	−62.75	Yes		
305.898−0.029C	199.35	−62.75	Yes		
305.923−0.097	199.42	−62.82	No	Yes	
305.924+0.034	199.39	−62.69	Yes		
305.928−0.185	199.45	−62.90	Yes		
305.984−0.078	199.55	−62.79	Yes		
306.037−0.120	199.67	−62.83	Yes		
306.090−0.095	199.78	−62.80	No	Yes	
306.188−0.246	200.03	−62.94	Yes		

continued on next page

IRDC Name	Right Ascension 2000.0 (°)	Declination 2000.0 (°)	8 μm source?	24 μm source?	Additional comments
306.190−0.214	200.03	−62.90	Yes		
306.230−0.007	200.07	−62.69	Yes		
306.230−0.565	200.20	−63.25	Yes		
306.237−0.559	200.22	−63.24	Yes		
306.309−0.036	200.24	−62.71	Yes		
306.324−0.053	200.28	−62.73	Yes		
306.451+0.049	200.53	−62.61	Yes		
306.495+0.070	200.62	−62.59	Yes		
306.531+0.022	200.71	−62.63	Yes		
306.614−0.161	200.94	−62.80	Yes		
306.627−0.168	200.97	−62.81			No distinct core
306.664−0.209	201.06	−62.84	Yes		
306.780−0.406	201.37	−63.02	Yes		
306.841−0.070	201.40	−62.68	Yes		
307.150−0.776	202.29	−63.34	Yes		
307.495+0.660	202.57	−61.87	No	No	
307.567−0.689	203.18	−63.19	Yes		
307.751−0.838	203.64	−63.31	Yes		
307.873+0.079	203.57	−62.38	Yes		
308.123−0.332	204.25	−62.74	Yes		
308.138−0.454	204.33	−62.86	Yes		
308.307−0.027	204.53	−62.41	Yes		
308.323+0.078	204.52	−62.30	Yes		
308.338+0.082	204.55	−62.30	Yes		
308.378+0.190	204.60	−62.18	Yes		
308.386+0.211	204.60	−62.16	Yes		
308.397−0.175	204.78	−62.54	Yes		
308.458+0.025	204.83	−62.33	Yes		
308.512+0.025	204.94	−62.32	No	No	Confused at 500 μm
308.588+0.763	204.81	−61.58	Yes		
308.641−0.097	205.27	−62.42	No	Yes	
308.650−0.437	205.43	−62.75	No	Yes	
308.662−0.065	205.30	−62.38	No	Yes	
308.781+0.091	205.49	−62.21	Yes		
308.792−0.434	205.73	−62.72	Yes		
308.891−0.135	205.81	−62.41			No distinct core
308.943+0.068	205.83	−62.20	Yes		
308.949−0.457	206.08	−62.71	Yes		
308.968−0.115	205.97	−62.37	Yes		
308.969+0.203	205.83	−62.06	Yes		
308.972−0.196	206.01	−62.45	Yes		
308.972−0.244	206.03	−62.50			No distinct core
308.985−0.459	206.15	−62.70	Yes		
308.993−0.180	206.05	−62.43	No	No	Confused at 500 μm
308.997−0.261	206.09	−62.51	No	Yes	
309.003−0.187	206.07	−62.44	Yes		
309.004−0.089	206.03	−62.34	Yes		
309.013−0.732	206.34	−62.97	Yes		
309.014−0.415	206.20	−62.66	Yes		
309.019−0.270	206.14	−62.51	Yes		
309.028−0.412	206.22	−62.65	Yes		
309.045−0.044	206.10	−62.29	Yes		
309.045−0.178	206.16	−62.42	Yes		
309.046−0.139	206.14	−62.38			No distinct core
309.058−0.027	206.12	−62.27	No	Yes	
309.068−0.244	206.23	−62.48	Yes		
309.079−0.208	206.24	−62.44	No	No	
309.085−0.146	206.23	−62.38	Yes		
309.101−0.074	206.23	−62.30	Yes		

continued on next page

IRDC Name	Right Ascension 2000.0 (°)	Declination 2000.0 (°)	8 μm source?	24 μm source?	Additional comments
309.111−0.298	206.35	−62.52	No	No	
309.117−0.484	206.45	−62.70	Yes		
309.124−0.993	206.70	−63.20	Yes		
309.124+0.112	206.20	−62.12	No	Yes	
309.129−0.144	206.32	−62.37	Yes		
309.131−0.191	206.34	−62.41	Yes		
309.136−0.165	206.34	−62.39	Yes		
309.146−0.491	206.51	−62.70	Yes		
309.154−0.550	206.56	−62.76	Yes		
309.154+0.122	206.25	−62.10	No	Yes	
309.157−0.345	206.47	−62.56	Yes		
309.160−0.223	206.42	−62.44	Yes		
309.171−0.147	206.41	−62.36	Yes		
309.178−0.552	206.61	−62.76	Yes		
309.219−0.654	206.74	−62.85			No distinct core
309.222−0.545	206.70	−62.74	Yes		
309.238−0.228	206.59	−62.43	Yes		
309.242−0.214	206.59	−62.41	Yes		
309.242+0.951	206.08	−61.27	No	No	Confused at 500 μm
309.254−0.620	206.80	−62.81			No distinct core
309.267−0.557	206.80	−62.74	No	Yes	
309.292−0.197	206.69	−62.38	Yes		
309.304−0.578	206.89	−62.75	No	Yes	
309.306−0.615	206.91	−62.79	Yes		
309.308−0.213	206.73	−62.40	Yes		
309.311−0.513	206.87	−62.69	Yes		
309.334−0.643	206.98	−62.81	Yes		
309.346−0.706	207.04	−62.87			No distinct core
309.362−0.628	207.04	−62.79	Yes		
309.374−0.093	206.81	−62.27	Yes		
309.374−0.622	207.06	−62.78	Yes		
309.392−0.410	207.00	−62.57	Yes		
309.401+0.465	206.61	−61.71	Yes		
309.409−0.574	207.11	−62.73	No	Yes	
309.418+0.973	206.43	−61.21			No distinct core
309.420−0.641	207.17	−62.79			No distinct core
309.434−0.661	207.21	−62.81			No distinct core
309.440−0.566	207.17	−62.71	Yes		
309.444−0.741	207.27	−62.88	Yes		
309.452−0.345	207.09	−62.49	Yes		
309.488−0.679	207.33	−62.81	Yes		
309.509−0.650	207.36	−62.78	Yes		
309.651+0.080	207.31	−62.04	Yes		
309.666−0.749	207.74	−62.84	No	No	Confused at 500 μm
309.671−0.829	207.80	−62.92	Yes		
309.759−0.438	207.79	−62.52	Yes		
309.759−0.471	207.80	−62.55	Yes		
309.781+0.381	207.44	−61.71	Yes		
309.894+0.647	207.54	−61.43	Yes		
309.903+0.230	207.76	−61.83	Yes		
309.915+0.323	207.74	−61.74	Yes		
309.916+0.493	207.66	−61.57	Yes		
309.950+0.391	207.78	−61.66	Yes		
309.967+0.595	207.71	−61.46	Yes		
309.975+0.301	207.87	−61.75	Yes		
309.990+0.435	207.84	−61.61	Yes		
309.994−0.230	208.18	−62.26	No	Yes	
310.013+0.485	207.86	−61.56	Yes		
310.024+0.302	207.97	−61.73			No distinct core

continued on next page

IRDC Name	Right Ascension 2000.0 (°)	Declination 2000.0 (°)	8 μm source?	24 μm source?	Additional comments
310.037−0.587	208.45	−62.60	Yes		
310.064−0.235	208.32	−62.25	No	Yes	
310.069+0.393	208.02	−61.63	Yes		
310.080+0.296	208.09	−61.73	Yes		
310.087+0.712	207.90	−61.32	Yes		
310.089+0.303	208.11	−61.72	Yes		
310.090−0.283	208.40	−62.29	Yes		
310.091−0.268	208.40	−62.27	Yes		
310.103+0.714	207.93	−61.31			No distinct core
310.132+0.379	208.16	−61.63	Yes		
310.136+0.399	208.15	−61.61			No distinct core
310.148+0.368	208.19	−61.64	Yes		
310.159+0.703	208.05	−61.31	Yes		
310.166+0.697	208.07	−61.32	Yes		
310.173+0.519	208.17	−61.49			No distinct core
310.173+0.719	208.07	−61.29	Yes		
310.183+0.469	208.22	−61.53	Yes		
310.193+0.414	208.26	−61.59	Yes		
310.198+0.320	208.32	−61.68	Yes		
310.199+0.430	208.27	−61.57	Yes		
310.209+0.042	208.48	−61.94	No	Yes	
310.221−0.586	208.83	−62.55	No	No	Confused at 500 μm
310.222+0.076	208.49	−61.91	No	Yes	
310.228+0.234	208.42	−61.75	Yes		
310.229+0.275	208.41	−61.71	No	No	Confused at 500 μm
310.231+0.381	208.36	−61.61	Yes		
310.243+0.403	208.37	−61.58			No distinct core
310.246+0.493	208.33	−61.50			No distinct core
310.248+0.473	208.35	−61.51	Yes		
310.297+0.705	208.33	−61.28	No	No	
310.319−0.546	209.02	−62.49	No	No	Confused at 500 μm
310.327−0.279	208.89	−62.23	Yes		
310.350−0.506	209.06	−62.44	Yes		
310.355−0.548	209.10	−62.48			No distinct core
310.362−0.563	209.12	−62.49			No distinct core
310.364−0.578	209.13	−62.51	Yes		
310.398−0.289	209.05	−62.22	No	Yes	
310.417+0.108	208.88	−61.83			No distinct core
310.474−0.460	209.30	−62.37	Yes		
310.482−0.095	209.12	−62.01	No	Yes	
310.495−0.515	209.37	−62.41	Yes		
310.523−0.036	209.17	−61.94	Yes		
310.526−0.066	209.19	−61.97	Yes		
310.542−0.480	209.45	−62.37	No	Yes	
310.581−0.070	209.31	−61.96	No	Yes	
310.598+0.725	208.93	−61.19	Yes		
310.600+0.688	208.95	−61.22	Yes		
310.601−0.599	209.64	−62.47			No distinct core
310.604+0.591	209.01	−61.31			No distinct core
310.613−0.613	209.67	−62.48	Yes		
310.613+0.765	208.94	−61.14			No distinct core
310.619−0.083	209.40	−61.96	Yes		
310.681+0.484	209.22	−61.40	Yes		
310.686+0.466	209.24	−61.42	Yes		
310.696+0.017	209.50	−61.85	Yes		
310.717−0.547	209.85	−62.39	Yes		
310.822+0.770	209.35	−61.09	Yes		
310.868+0.472	209.60	−61.36	Yes		
310.948+0.723	209.63	−61.10	Yes		

continued on next page

IRDC Name	Right Ascension 2000.0 (°)	Declination 2000.0 (°)	8 μm source?	24 μm source?	Additional comments
310.952−0.691	210.43	−62.46	Yes		
310.974+1.010	209.53	−60.82			No distinct core
310.982−0.243	210.23	−62.02	No	Yes	
311.000+0.738	209.73	−61.07	Yes		
311.016+0.434	209.92	−61.36	Yes		
311.020−0.326	210.35	−62.09	Yes		
311.021+0.467	209.91	−61.33	No	Yes	
311.024+0.895	209.69	−60.91	Yes		
311.033−0.291	210.36	−62.06	No	Yes	
311.042+0.689	209.84	−61.11	Yes		
311.046+0.420	209.99	−61.37	Yes		
311.051+0.392	210.02	−61.39	No	Yes	
311.051+0.792	209.80	−61.01			No distinct core
311.055+0.859	209.77	−60.94	Yes		
311.061+0.425	210.02	−61.36			No distinct core
311.065+0.696	209.88	−61.10	No	Yes	
311.065+0.816	209.81	−60.98	Yes		
311.086+0.370	210.10	−61.40	No	Yes	
311.088+0.403	210.08	−61.37	No	Yes	
311.094+0.733	209.92	−61.05	No	Yes	
311.107+0.411	210.12	−61.36	Yes		
311.131+0.790	209.96	−60.99	Yes		
311.167+1.000	209.92	−60.78	Yes		
311.178+0.155	210.40	−61.59	No	Yes	
311.181+0.785	210.06	−60.98	Yes		
311.191−0.586	210.86	−62.30	Yes		
311.202+0.722	210.14	−61.03	Yes		
311.209−0.605	210.91	−62.31	Yes		
311.246+0.023	210.62	−61.70	Yes		
311.285−0.113	210.78	−61.82			No distinct core
311.335−0.349	211.01	−62.03	Yes		
311.352+0.356	210.64	−61.35	Yes		
311.432−0.473	211.29	−62.12	Yes		
311.570−0.208	211.41	−61.83	No	Yes	
311.641−0.609	211.80	−62.19			No distinct core
311.670−0.687	211.91	−62.26	Yes		
311.670+0.278	211.32	−61.33	Yes		
311.721−0.335	211.79	−61.91			No distinct core
311.747−0.691	212.07	−62.24	No	Yes	
311.756−0.673	212.08	−62.22	No	No	Confused at 500 μm
311.801+0.029	211.73	−61.53			No distinct core
311.823−0.805	212.30	−62.33	No	No	Confused at 500 μm
311.825−0.738	212.26	−62.26	No	Yes	
311.832−0.761	212.29	−62.28	Yes		
311.835−0.699	212.25	−62.22			No distinct core
311.848−0.382	212.08	−61.92	Yes		
311.856+0.244	211.72	−61.31	Yes		
311.857−0.841	212.39	−62.35	No	No	Confused at 500 μm
311.875+0.026	211.88	−61.52	Yes		
311.893+0.375	211.71	−61.18			No distinct core
311.903−0.866	212.50	−62.36	Yes		
311.903+0.234	211.81	−61.31	Yes		
311.937+0.353	211.81	−61.19			No distinct core
311.943+0.137	211.95	−61.39	Yes		
311.992−0.544	212.48	−62.03	Yes		
311.995−0.168	212.24	−61.67	Yes		
312.012−0.590	212.55	−62.07	Yes		
312.022−0.219	212.33	−61.71	No	Yes	
312.028−0.553	212.56	−62.03	Yes		

continued on next page

IRDC Name	Right Ascension 2000.0 (°)	Declination 2000.0 (°)	8 μm source?	24 μm source?	Additional comments
312.034−0.739	212.69	−62.20			No distinct core
312.045−0.467	212.53	−61.94	Yes		
312.046−0.576	212.61	−62.04			No distinct core
312.050−0.564	212.61	−62.03			No distinct core
312.063−0.529	212.61	−61.99	Yes		
312.068−0.529	212.62	−61.99	Yes		
312.070−0.468	212.59	−61.93			No distinct core
312.088−0.525	212.66	−61.98	No	No	Confused at 500 μm
312.089−0.619	212.72	−62.07	No	Yes	
312.103−0.523	212.69	−61.97			No distinct core
312.116−0.625	212.78	−62.07	No	No	Confused at 500 μm
312.122−0.040	212.42	−61.51	Yes		
312.126−0.765	212.89	−62.20	Yes		
312.165−0.205	212.61	−61.65	Yes		
312.168−0.077	212.54	−61.53	Yes		
312.174−0.032	212.52	−61.48	Yes		
312.197−0.156	212.64	−61.60	Yes		
312.214+0.740	212.12	−60.73	Yes		
312.216−0.857	213.14	−62.26			No distinct core
312.232−0.103	212.68	−61.54	Yes		
312.235−0.788	213.13	−62.19	Yes		
312.248+0.040	212.62	−61.39	Yes		
312.266+0.759	212.21	−60.70	Yes		
312.267+0.049	212.65	−61.38	Yes		
312.276−0.802	213.22	−62.19			No distinct core
312.295+0.089	212.68	−61.33	Yes		
312.295+0.737	212.28	−60.71	No	No	Confused at 500 μm
312.332−0.086	212.87	−61.49	Yes		
312.356−0.029	212.88	−61.43	Yes		
312.358−0.285	213.05	−61.67	Yes		
312.376−0.123	212.98	−61.51			No distinct core
312.377−0.301	213.10	−61.68	No	Yes	
312.380−0.309	213.11	−61.69	Yes		
312.385−0.104	212.99	−61.49			No distinct core
312.393−0.333	213.15	−61.71	Yes		
312.396−0.487	213.26	−61.85	Yes		
312.397+0.934	212.36	−60.50	No	No	Confused at 500 μm
312.476−0.053	213.14	−61.41	Yes		
312.505−0.361	213.39	−61.70	Yes		
312.508+0.008	213.16	−61.34			No distinct core
312.513−0.017	213.19	−61.37	Yes		
313.560+0.149	215.12	−60.87	No	Yes	
313.613−0.188	215.46	−61.17	Yes		
313.627−0.212	215.51	−61.19	No	Yes	
313.629−0.073	215.41	−61.06	Yes		
313.630+0.267	215.18	−60.74			No distinct core
313.637−0.359	215.63	−61.32	No	No	Confused at 500 μm
313.637−0.803	215.96	−61.74	Yes		
313.693−0.155	215.60	−61.11			No distinct core
313.701−0.531	215.88	−61.46	No	Yes	
313.726−0.310	215.77	−61.25	No	Yes	
313.738−0.108	215.65	−61.05	Yes		
313.744+0.391	215.31	−60.58	Yes		
313.753−0.085	215.66	−61.03			No distinct core
313.759−0.127	215.71	−61.06	Yes		
313.760+0.366	215.36	−60.60	No	No	Confused at 500 μm
313.765−0.496	215.98	−61.41	Yes		
313.765+0.230	215.46	−60.73	No	No	Confused at 500 μm
313.768+0.211	215.48	−60.74	No	Yes	

continued on next page

IRDC Name	Right Ascension 2000.0 (°)	Declination 2000.0 (°)	8 μm source?	24 μm source?	Additional comments
313.773+0.254	215.46	−60.70	Yes		
313.778−0.185	215.78	−61.11	Yes		
313.778−0.327	215.89	−61.24	Yes		
313.782+0.208	215.51	−60.74			No distinct core
313.783−0.170	215.78	−61.10			No distinct core
313.790−0.194	215.81	−61.12	Yes		
313.798+0.049	215.66	−60.88	Yes		
313.800+0.202	215.55	−60.74	Yes		
313.806−0.247	215.88	−61.16	Yes		
313.809−0.278	215.91	−61.19	Yes		
313.815+0.359	215.47	−60.59	No	No	Confused at 500 μm
313.817−0.271	215.92	−61.18			No distinct core
313.826−0.293	215.95	−61.20	Yes		
313.828+0.684	215.27	−60.28	Yes		
313.845+0.188	215.65	−60.74	Yes		
313.852−0.226	215.96	−61.12	No	Yes	
313.872+0.052	215.79	−60.86	No	No	Confused at 160 μm
313.887+0.151	215.75	−60.76	Yes		
313.935−0.033	215.98	−60.91	No	Yes	
313.938+0.064	215.91	−60.82	Yes		
313.946−0.016	215.99	−60.89	No	Yes	
313.986+0.037	216.03	−60.83	Yes		
313.994−0.234	216.24	−61.08	Yes		
314.083−0.461	216.58	−61.26	Yes		
314.087−0.113	216.33	−60.94	Yes		
314.087+0.372	215.98	−60.48			No distinct core
314.128−0.068	216.38	−60.88	Yes		
314.146−0.085	216.42	−60.89	Yes		
314.175−0.073	216.47	−60.87	Yes		
314.214−0.309	216.72	−61.07	Yes		
314.271+0.925	215.94	−59.90	No	No	Confused at 500 μm
314.282+0.055	216.58	−60.71	No	Yes	
314.296+0.035	216.62	−60.72	Yes		
314.315−0.047	216.72	−60.79	No	No	Confused at 500 μm
314.324−0.393	216.99	−61.11			No distinct core
314.325−0.177	216.83	−60.91	Yes		
314.327−0.044	216.74	−60.79	No	Yes	
314.327+0.028	216.69	−60.72			No distinct core
314.340+0.021	216.71	−60.72			No distinct core
314.350−0.025	216.77	−60.76	Yes		
314.372+0.933	216.12	−59.85	No	No	Confused at 500 μm
314.373+0.096	216.72	−60.64	Yes		
314.382−0.084	216.87	−60.80	Yes		
314.383+0.942	216.14	−59.84	No	No	Confused at 500 μm
314.392+0.069	216.78	−60.66			No distinct core
314.393+0.112	216.75	−60.61	Yes		
314.397−0.023	216.86	−60.74	No	Yes	
314.400−0.039	216.88	−60.75	Yes		
314.400−0.071	216.90	−60.78	Yes		
314.402+0.049	216.81	−60.67	No	Yes	
314.406−0.016	216.87	−60.73	Yes		
314.412+0.138	216.77	−60.58	Yes		
314.430+0.008	216.90	−60.70	No	Yes	
314.432+0.153	216.79	−60.56	Yes		
314.436−0.013	216.92	−60.72	No	No	Confused at 500 μm
314.461−0.030	216.98	−60.72	Yes		
314.563+0.185	217.02	−60.49	Yes		
314.582+0.703	216.68	−60.00	No	No	Confused at 500 μm
314.592−0.294	217.43	−60.92	No	No	Confused at 500 μm

continued on next page

IRDC Name	Right Ascension 2000.0 (°)	Declination 2000.0 (°)	8 μm source?	24 μm source?	Additional comments
314.597−0.316	217.46	−60.94	No	No	Confused at 500 μm
314.603−0.011	217.24	−60.65	Yes		
314.612−0.326	217.49	−60.94	Yes		
314.629+0.068	217.23	−60.57	No	No	Confused at 500 μm
314.631−0.327	217.53	−60.94	Yes		
314.634+0.150	217.18	−60.49	Yes		
314.639−0.308	217.53	−60.92			No distinct core
314.644+0.085	217.24	−60.55	Yes		
314.649−0.292	217.54	−60.90	Yes		
314.663+0.221	217.18	−60.42	Yes		
314.673−0.292	217.59	−60.89	Yes		
314.697−0.308	217.64	−60.90	Yes		
314.701+0.183	217.28	−60.44	No	No	
314.710+0.201	217.28	−60.42			No distinct core
314.713−0.313	217.68	−60.89	Yes		
314.720+0.243	217.27	−60.37			No distinct core
314.723−0.292	217.68	−60.87	Yes		
314.730−0.064	217.52	−60.66	Yes		
314.737−0.277	217.70	−60.85	No	No	Confused at 500 μm
314.738−0.322	217.73	−60.89	Yes		
314.742−0.186	217.64	−60.76			No distinct core
314.746−0.171	217.63	−60.75	Yes		
314.755−0.373	217.81	−60.93			No distinct core
314.756−0.382	217.81	−60.94			No distinct core
314.758−0.350	217.79	−60.91			No distinct core
314.760−0.368	217.81	−60.93			No distinct core
314.760+0.216	217.37	−60.38	Yes		
314.763−0.028	217.56	−60.61	No	No	Confused at 500 μm
314.768−0.333	217.80	−60.89	No	No	Confused at 160 μm
314.770+0.212	217.39	−60.38	No	No	Confused at 500 μm
314.777−0.055	217.60	−60.63			No distinct core
314.784−0.358	217.85	−60.91	Yes		
314.800−0.080	217.66	−60.65	Yes		
314.801+0.088	217.54	−60.49			No distinct core
314.806−0.172	217.75	−60.73	No	Yes	
314.808−0.643	218.12	−61.16	Yes		
314.828−0.188	217.80	−60.73			No distinct core
314.848−0.388	217.99	−60.91	Yes		
314.869+0.093	217.66	−60.46	No	No	Confused at 500 μm
314.878−0.143	217.86	−60.67	Yes		
314.889−0.149	217.89	−60.68			No distinct core
314.901−0.298	218.02	−60.81	Yes		
314.911−0.292	218.04	−60.80			No distinct core
314.916−0.622	218.31	−61.10	Yes		
314.935+0.542	217.45	−60.02	No	No	Confused at 500 μm
314.942−0.508	218.27	−60.99	Yes		
314.942−0.605	218.34	−61.08	No	No	Confused at 500 μm
314.954+0.539	217.49	−60.01	Yes		
314.963−0.187	218.06	−60.68			No distinct core
314.970−0.214	218.09	−60.71			No distinct core
314.970−0.324	218.18	−60.81			No distinct core
314.978+0.038	217.91	−60.47	No	Yes	
314.988−0.232	218.14	−60.72	Yes		
315.005−0.076	218.05	−60.56	No	Yes	
315.010−0.139	218.11	−60.62	Yes		
315.015+0.046	217.97	−60.45	No	Yes	
315.016−0.158	218.13	−60.64	Yes		
315.017+0.028	217.99	−60.46			No distinct core
315.036+0.200	217.9	−60.30	Yes		

continued on next page

IRDC Name	Right Ascension 2000.0 (°)	Declination 2000.0 (°)	8 μm source?	24 μm source?	Additional comments
315.039−0.173	218.19	−60.64			No distinct core
315.049+0.181	217.93	−60.31	Yes		
315.150−0.319	218.51	−60.73	No	No	Confused at 500 μm
315.151−0.328	218.52	−60.74	Yes		
315.214−0.291	218.61	−60.68	Yes		
315.518−0.920	219.70	−61.14	Yes		
315.686−0.598	219.75	−60.78	Yes		
315.696−0.555	219.73	−60.74	No	No	Confused at 500 μm
315.933−0.659	220.26	−60.73	No	No	Confused at 500 μm
315.967−0.606	220.28	−60.67			No distinct core
315.971−0.599	220.28	−60.66			No distinct core
315.997−0.590	220.32	−60.65	Yes		
316.003−0.769	220.48	−60.81			No distinct core
316.013−0.673	220.42	−60.71			No distinct core
316.040−0.618	220.42	−60.65	No	No	Confused at 500 μm
316.293−0.364	220.68	−60.32	Yes		
316.306−0.330	220.67	−60.28	No	No	Confused at 500 μm
316.313−0.350	220.70	−60.30			No distinct core
316.320−0.391	220.75	−60.33	Yes		
316.347−0.545	220.93	−60.46	Yes		
316.389−0.470	220.94	−60.37	Yes		
316.402−0.463	220.96	−60.36	Yes		
316.402−0.675	221.14	−60.55	No	No	Confused at 500 μm
316.416−0.455	220.98	−60.35	Yes		
316.424−0.478	221.01	−60.37	No	Yes	
316.424−0.633	221.15	−60.51	No	No	Confused at 500 μm
316.429−0.492	221.04	−60.38			No distinct core
316.468−0.730	221.31	−60.58			No distinct core
316.471−0.271	220.92	−60.16	Yes		
316.473−0.517	221.14	−60.38			No distinct core
316.482−0.230	220.91	−60.12	No	Yes	
316.483+0.273	220.50	−59.66	No	No	Confused at 500 μm
316.506+0.274	220.54	−59.65	No	No	Confused at 500 μm
316.513−0.223	220.96	−60.10	Yes		
316.526−0.252	221.01	−60.12	Yes		
316.536+0.059	220.77	−59.83	Yes		
316.553+0.045	220.81	−59.84	Yes		
316.575+0.067	220.83	−59.81	No	Yes	
316.579−0.217	221.08	−60.06	Yes		
316.591+0.068	220.86	−59.80			No distinct core
316.634−0.432	221.36	−60.24	Yes		
316.640−0.408	221.35	−60.21	Yes		
316.647−0.367	221.33	−60.17			No distinct core
316.656−0.268	221.26	−60.08	No	Yes	
316.724+0.130	221.05	−59.69	No	Yes	
316.804+0.144	221.18	−59.64			Stripy at 250 μm
316.828+0.100	221.26	−59.67	Yes		
316.902+0.174	221.33	−59.57	No	Yes	
316.903+0.459	221.09	−59.31	No	Yes	
316.920+0.228	221.32	−59.52			No distinct core
316.944−0.014	221.56	−59.73	Yes		
316.950+0.131	221.45	−59.59			No distinct core
317.048+0.432	221.37	−59.28			No distinct core
317.074−0.087	221.86	−59.74			Stripy at 250 μm
317.397+0.198	222.19	−59.34	No	Yes	
317.400−0.161	222.50	−59.66	Yes		
317.430−0.371	222.74	−59.84	No	Yes	
317.445−0.059	222.49	−59.55	No	Yes	
317.452−0.026	222.48	−59.52	No	Yes	

continued on next page

IRDC Name	Right Ascension 2000.0 (°)	Declination 2000.0 (°)	8 μm source?	24 μm source?	Additional comments
317.461−0.948	223.31	−60.34	No	No	Confused at 500 μm
317.470−0.211	222.67	−59.67	Yes		
317.480−0.684	223.11	−60.09			No distinct core
317.562+0.099	222.56	−59.35	No	Yes	
317.564−0.094	222.74	−59.53	Yes		
317.574−0.824	223.41	−60.18			No distinct core
317.580−0.098	222.77	−59.52	Yes		
317.591−0.835	223.44	−60.18			No distinct core
317.596−0.837	223.46	−60.18			No distinct core
317.614+0.072	222.68	−59.36	No	No	Confused at 500 μm
317.628−0.820	223.50	−60.15			No distinct core
317.649+0.012	222.79	−59.39	No	Yes	
317.657+0.105	222.73	−59.31			No distinct core
317.742+0.120	222.86	−59.26	No	No	Confused at 500 μm
317.783−0.078	223.11	−59.42	Yes		
317.849+0.485	222.73	−58.88	Yes		
317.866−0.306	223.46	−59.58	Yes		
317.870−0.149	223.32	−59.44	Yes		
317.876−0.175	223.36	−59.46	No	No	Confused at 500 μm
317.910−0.007	223.27	−59.30	No	No	Confused at 500 μm
317.942+0.013	223.31	−59.26	No	No	Confused at 500 μm
318.014+0.052	223.40	−59.19	Yes		
318.015+0.064	223.39	−59.18	Yes		
318.039+0.158	223.35	−59.09			No distinct core
318.058+0.134	223.40	−59.10			No distinct core
318.063+0.174	223.37	−59.06	No	Yes	
318.080+0.114	223.46	−59.11			No distinct core
318.086+0.097	223.48	−59.12			No distinct core
318.103+0.107	223.50	−59.10	No	Yes	
318.133−0.664	224.25	−59.78	Yes		
318.157−0.335	223.99	−59.47	No	Yes	
318.187−0.358	224.07	−59.48	Yes		
318.199+0.076	223.70	−59.09			No distinct core
318.227+0.031	223.79	−59.12			No distinct core
318.228−0.739	224.49	−59.80	No	Yes	
318.306−0.131	224.07	−59.23	Yes		
318.306−0.732	224.62	−59.76	No	Yes	
318.343+0.309	223.74	−58.82	No	No	Confused at 500 μm
318.390−0.152	224.23	−59.21	Yes		
318.404+0.394	223.77	−58.71	Yes		
318.419−0.085	224.22	−59.13	Yes		
318.499−0.278	224.54	−59.27	Yes		
318.550−0.274	224.62	−59.24			No distinct core
318.553−0.165	224.53	−59.14	No	Yes	
318.563−0.174	224.55	−59.14			No distinct core
318.566−0.184	224.57	−59.15	No	No	Confused at 500 μm
318.573−0.173	224.57	−59.14			No distinct core
318.573+0.642	223.84	−58.41	No	No	
318.585−0.206	224.62	−59.16	Yes		
318.614+0.301	224.21	−58.70	No	No	Confused at 500 μm
318.617−0.342	224.80	−59.27	Yes		
318.655+0.666	223.96	−58.36	No	No	Confused at 500 μm
318.677+0.652	224.01	−58.36	No	No	Confused at 500 μm
318.688−0.783	225.33	−59.62			No distinct core
318.689−0.128	224.73	−59.04	Yes		
318.703+0.673	224.03	−58.33	Yes		
318.727−0.687	225.31	−59.52	Yes		
318.738−0.098	224.78	−58.99			No distinct core
318.755−0.011	224.73	−58.91	No	No	Confused at 500 μm

continued on next page

IRDC Name	Right Ascension 2000.0 (°)	Declination 2000.0 (°)	8 μm source?	24 μm source?	Additional comments
318.757−0.002	224.73	−58.90	Yes		
318.763−0.448	225.15	−59.29	No	Yes	
318.778−0.175	224.92	−59.04	Yes		
318.785−0.397	225.14	−59.24	Yes		
318.802+0.416	224.43	−58.51	No	No	
318.875−0.272	225.18	−59.08	No	Yes	
318.895−0.244	225.19	−59.05	No	No	Confused at 500 μm
318.907−0.239	225.20	−59.04	No	Yes	
318.916−0.284	225.26	−59.07	No	No	
318.932−0.266	225.27	−59.05	Yes		
318.937−0.043	225.07	−58.85			Stripy at 250 μm
318.997−0.224	225.34	−58.98	No	No	Confused at 500 μm
319.000+0.164	224.99	−58.64	Yes		
319.094−0.491	225.76	−59.17	No	No	Confused at 160 μm
319.263+0.851	224.81	−57.91			No distinct core
319.334+0.828	224.95	−57.90	Yes		
319.374+0.897	224.96	−57.82	No	Yes	
319.402+0.863	225.03	−57.83	No	No	Confused at 500 μm
319.420+0.824	225.10	−57.86	No	No	Confused at 500 μm
319.460+0.835	225.15	−57.83	Yes		
319.644+0.812	225.48	−57.76	Yes		
319.728−0.873	227.20	−59.19			No distinct core
319.740−0.874	227.22	−59.18	Yes		
319.821−0.388	226.89	−58.72	Yes		
319.828+0.670	225.91	−57.80	Yes		
319.904−0.256	226.90	−58.57	Yes		
319.988+0.101	226.70	−58.21	Yes		
319.998+0.706	226.15	−57.68			No distinct core
320.014+0.724	226.16	−57.66			No distinct core
320.022+0.709	226.19	−57.67	No	No	Confused at 500 μm
320.052+0.700	226.25	−57.66	No	No	Confused at 500 μm
320.074+0.683	226.30	−57.67	No	Yes	
320.146+0.077	226.98	−58.16	Yes		
320.234+0.331	226.89	−57.89	No	No	Confused at 500 μm
320.235+0.346	226.87	−57.88	No	Yes	
320.271+0.249	227.02	−57.95			No distinct core
320.271+0.293	226.98	−57.91	Yes		
320.284+0.270	227.03	−57.92			No distinct core
320.287−0.538	227.81	−58.62	Yes		
320.302+0.217	227.10	−57.96			No distinct core
320.304+0.398	226.94	−57.80			No distinct core
320.317−0.443	227.76	−58.52	Yes		
320.321+0.213	227.14	−57.95			No distinct core
320.328−0.430	227.77	−58.50	Yes		
320.328+0.585	226.80	−57.63	Yes		
320.338+0.907	226.52	−57.34	No	No	Confused at 500 μm
320.387+0.141	227.31	−57.98	No	Yes	
320.389+0.123	227.33	−58.00	Yes		
320.469−0.204	227.78	−58.24	Yes		
320.551−0.206	227.92	−58.20	No	No	Confused at 500 μm
320.565+0.429	227.33	−57.64	Yes		
320.574−0.187	227.93	−58.17	No	No	Confused at 500 μm
320.590+0.497	227.31	−57.57	No	No	Confused at 500 μm
320.605+0.458	227.37	−57.60	No	No	Confused at 500 μm
320.629−0.521	228.35	−58.43	Yes		
320.639+0.331	227.54	−57.69	Yes		
320.773−0.448	228.51	−58.29	No	No	Confused at 500 μm
320.786+0.697	227.43	−57.30	No	No	Confused at 160 μm
320.864−0.362	228.58	−58.17	No	Yes	

continued on next page

IRDC Name	Right Ascension 2000.0 (°)	Declination 2000.0 (°)	8 μm source?	24 μm source?	Additional comments
320.879−0.397	228.64	−58.19	Yes		
320.884−0.575	228.82	−58.34			No distinct core
320.993−0.196	228.62	−57.96	Yes		
321.011−0.477	228.93	−58.19	No	Yes	
321.213−0.593	229.37	−58.18			No distinct core
321.313+0.348	228.60	−57.33	No	No	Confused at 500 μm
321.322−0.372	229.32	−57.94	No	No	Confused at 500 μm
321.332+0.881	228.13	−56.86	Yes		
321.336−0.373	229.35	−57.93	No	No	Confused at 500 μm
321.336−0.393	229.37	−57.95	No	No	Confused at 500 μm
321.341−0.381	229.36	−57.94	No	No	Confused at 500 μm
321.356+0.142	228.87	−57.48			No distinct core
321.397+0.934	228.18	−56.78	No	No	Confused at 500 μm
321.409+0.515	228.60	−57.14	Yes		
321.429+0.107	229.02	−57.47			No distinct core
321.468+0.774	228.44	−56.88	Yes		
321.472+0.574	228.64	−57.05	No	No	Confused at 500 μm
321.557+0.029	229.30	−57.47	No	No	Confused at 500 μm
321.560+0.116	229.22	−57.40	No	No	Confused at 500 μm
321.617+0.055	229.37	−57.42	Yes		
321.619+0.103	229.33	−57.38	Yes		
321.642+0.078	229.39	−57.39	Yes		
321.659+0.049	229.44	−57.40			No distinct core
321.670−0.016	229.52	−57.45	No	No	Confused at 500 μm
321.672+0.092	229.42	−57.36	Yes		
321.678+0.965	228.59	−56.61	No	No	
321.680+0.082	229.44	−57.36			No distinct core
321.688−0.015	229.55	−57.44			No distinct core
321.697+0.048	229.50	−57.38			No distinct core
321.721−0.010	229.60	−57.42	Yes		
321.725+0.830	228.79	−56.70			No distinct core
321.729−0.007	229.61	−57.41			No distinct core
321.736+0.804	228.83	−56.72	No	No	Confused at 500 μm
321.740+0.830	228.81	−56.70	No	No	Confused at 500 μm
321.746−0.629	230.26	−57.93	No	No	Confused at 500 μm
321.753+0.669A	228.99	−56.83	Yes		
321.753+0.669B	228.99	−56.83	No	No	
321.758+0.033	229.61	−57.36	Yes		
321.766+0.777	228.90	−56.73	No	No	Confused at 500 μm
321.818−0.605	230.35	−57.87	Yes		
321.892−0.059	229.92	−57.37			No distinct core
321.898−0.012	229.88	−57.33	No	No	Confused at 500 μm
321.899−0.234	230.10	−57.51	Yes		
321.950−0.064	230.01	−57.34	Yes		
321.950−0.092	230.04	−57.37			No distinct core
322.012−0.112	230.16	−57.35			No distinct core
322.023+0.851	229.23	−56.53			No distinct core
322.027−0.256	230.32	−57.46	Yes		
322.063−0.077	230.20	−57.29	Yes		
322.084−0.061	230.22	−57.27	Yes		
322.334+0.561A	229.99	−56.61	Yes		
322.334+0.561B	229.99	−56.61	No	No	
322.413−0.565	231.24	−57.51			No distinct core
322.518+0.404	230.42	−56.64	Yes		
322.626+0.652	230.34	−56.37	Yes		
322.632+0.029	230.97	−56.89	No	No	Confused at 500 μm
322.659+0.053	230.99	−56.86	No	No	Confused at 500 μm
322.666−0.588	231.65	−57.39	No	No	
322.680+0.032	231.04	−56.86	No	No	Confused at 500 μm

continued on next page

IRDC Name	Right Ascension 2000.0 (°)	Declination 2000.0 (°)	8 μm source?	24 μm source?	Additional comments
322.686+0.208	230.87	−56.71	No	No	Confused at 500 μm
322.795−0.569	231.83	−57.30	Yes		
322.813+0.801	230.48	−56.15	Yes		
322.822−0.780	232.09	−57.46	No	No	Confused at 500 μm
322.895+0.277	231.12	−56.54	Yes		
322.901+0.236	231.17	−56.57			No distinct core
322.905+0.223	231.19	−56.58	No	No	Confused at 500 μm
322.914+0.321	231.11	−56.49	No	No	
322.984+0.211	231.32	−56.55	Yes		
323.116−0.652	232.41	−57.19	No	No	Confused at 500 μm
323.122+0.050	231.69	−56.60	Yes		
323.142+0.173	231.60	−56.49	No	No	Confused at 500 μm
323.204+0.063	231.80	−56.55			No distinct core
323.212+0.315	231.56	−56.34	No	No	Confused at 500 μm
323.230−0.398	232.32	−56.92			No distinct core
323.238−0.406	232.34	−56.92			No distinct core
323.261−0.011	231.97	−56.58	Yes		
323.312−0.392	232.44	−56.86	Yes		
323.325−0.375	232.44	−56.84	Yes		
323.338−0.053	232.12	−56.57	No	No	Confused at 500 μm
323.424−0.441	232.65	−56.84	Yes		
323.479+0.099	232.18	−56.36	Yes		
323.483+0.502	231.78	−56.03	No	No	Confused at 500 μm
323.507−0.466	232.80	−56.81	Yes		
323.546+0.065	232.31	−56.35	Yes		
323.547−0.411	232.81	−56.75	Yes		
323.573+0.256	232.16	−56.18	No	No	Confused at 500 μm
323.621+0.275	232.21	−56.14	No	No	Confused at 500 μm
323.824+0.208	232.58	−56.08	Yes		
323.839+0.487	232.32	−55.84			No distinct core
323.845+0.052	232.77	−56.20	Yes		
323.870−0.250	233.12	−56.43			Stripy at 250 μm
323.893−0.516	233.43	−56.63	Yes		
323.931−0.287	233.25	−56.42	Yes		
323.934+0.410	232.54	−55.85			No distinct core
323.987+0.423	232.60	−55.81	Yes		
324.005+0.633	232.42	−55.63	No	No	Confused at 500 μm
324.048−0.425	233.57	−56.47	No	No	Confused at 500 μm
324.056+0.561	232.56	−55.66	No	No	Confused at 500 μm
324.067−0.428	233.60	−56.46	No	Yes	
324.079+0.447	232.71	−55.74	Yes		
324.100−0.576	233.80	−56.56	Yes		
324.103+0.167	233.03	−55.95	Yes		
324.110−0.425	233.66	−56.43	No	No	Confused at 500 μm
324.243+0.095	233.31	−55.93	Yes		
324.320+0.526	232.98	−55.53	Yes		
324.330+0.514	233.01	−55.54	Yes		
324.338+0.511	233.02	−55.54			No distinct core
324.466−0.462	234.22	−56.25			No distinct core
325.027+0.306	234.22	−55.30	Yes		
325.129−0.038	234.72	−55.52	Yes		
325.312−0.261	235.22	−55.59			No distinct core
325.434+0.468	234.63	−54.93	No	No	Confused at 500 μm
325.529+0.209	235.03	−55.08	No	No	Confused at 500 μm
325.635+0.459	234.92	−54.82			No distinct core
325.660+0.326	235.09	−54.91	No	No	Confused at 500 μm
325.742+0.530	234.99	−54.70	Yes		
325.794−0.228	235.86	−55.27	Yes		
325.813+0.469	235.15	−54.71	No	Yes	

continued on next page

IRDC Name	Right Ascension 2000.0 (°)	Declination 2000.0 (°)	8 μm source?	24 μm source?	Additional comments
325.838−0.225	235.92	−55.24	Yes		
325.873+0.245	235.47	−54.85			No distinct core
325.884+0.229	235.50	−54.85	Yes		
325.885−0.153	235.91	−55.16	No	No	Confused at 500 μm
325.908−0.005	235.78	−55.03	Yes		
325.913−0.084	235.87	−55.09	No	No	Confused at 500 μm
325.940+0.068	235.75	−54.95	No	No	Confused at 500 μm
325.958+0.075	235.77	−54.93	No	Yes	
326.057−0.314	236.32	−55.18	No	Yes	
326.154−0.511	236.67	−55.28	No	Yes	
326.310+0.428	235.88	−54.44	Yes		
326.311+0.542	235.76	−54.35	No	Yes	
326.322+0.458	235.87	−54.41	No	No	Confused at 500 μm
326.334+0.439	235.90	−54.42	No	No	Confused at 500 μm
326.337+0.461	235.88	−54.40	No	No	Confused at 500 μm
326.352+0.458	235.91	−54.39			No distinct core
326.356+0.444	235.93	−54.40	Yes		
326.369−0.200	236.63	−54.90	Yes		
326.376+0.488	235.91	−54.35	No	Yes	
326.382+0.366	236.04	−54.44	Yes		
326.384−0.197	236.64	−54.89	Yes		
326.394+0.847	235.56	−54.05	No	Yes	
326.400+0.715	235.70	−54.16	Yes		
326.409+0.594	235.84	−54.25	No	No	Confused at 500 μm
326.413+0.394	236.06	−54.40	Yes		
326.416+0.042	236.43	−54.68	Yes		
326.424+0.499	235.96	−54.31	No	No	Confused at 500 μm
326.434−0.149	236.66	−54.82	Yes		
326.453+0.757	235.73	−54.09	Yes		
326.458−0.092	236.63	−54.76			No distinct core
326.466−0.507	237.09	−55.08	No	Yes	
326.478−0.132	236.70	−54.78	Yes		
326.485−0.172	236.75	−54.81	Yes		
326.490+0.629	235.92	−54.17	Yes		
326.491−0.158	236.75	−54.79	No	Yes	
326.495+0.581	235.97	−54.20	No	No	
326.496+0.355	236.21	−54.38	Yes		
326.501−0.489	237.12	−55.04	Yes		
326.503−0.127	236.73	−54.76			No distinct core
326.509−0.125	236.74	−54.75			No distinct core
326.521+0.582	236.01	−54.19	Yes		
326.526+0.529	236.07	−54.23	Yes		
326.529−0.787	237.48	−55.26	Yes		
326.532−0.751	237.45	−55.23	Yes		
326.537+0.931	235.67	−53.90	No	No	Confused at 500 μm
326.539+0.942	235.66	−53.89	No	No	Confused at 500 μm
326.546+0.938	235.67	−53.89			No distinct core
326.549−0.228	236.90	−54.81	Yes		
326.557+0.314	236.34	−54.38	Yes		
326.560+0.924	235.71	−53.89	No	No	Confused at 500 μm
326.560+0.947	235.68	−53.87			No distinct core
326.575+0.952	235.70	−53.86	No	No	Confused at 500 μm
326.579+0.945	235.71	−53.86			No distinct core
326.590+0.941	235.73	−53.86			No distinct core
326.596+0.957	235.72	−53.84	No	No	Confused at 500 μm
326.598+0.835	235.85	−53.94			No distinct core
326.598+0.939	235.74	−53.86	Yes		
326.611+0.811	235.89	−53.95	Yes		
326.618−0.209	236.98	−54.75	Yes		

continued on next page

IRDC Name	Right Ascension 2000.0 (°)	Declination 2000.0 (°)	8 μm source?	24 μm source?	Additional comments
326.620−0.143	236.91	−54.70	No	No	
326.622+0.372	236.36	−54.29	Yes		
326.622+0.919	235.80	−53.86			No distinct core
326.632+0.951	235.77	−53.83	No	No	
326.634+0.978	235.75	−53.80			No distinct core
326.635−0.507	237.32	−54.98			No distinct core
326.635+0.421	236.33	−54.25			No distinct core
326.637+0.700	236.04	−54.02	Yes		
326.641+0.941	235.80	−53.83	Yes		
326.642+0.966	235.77	−53.81			No distinct core
326.643+0.917	235.83	−53.85	No	No	Confused at 500 μm
326.648−0.129	236.93	−54.67	Yes		
326.664+0.342	236.45	−54.29	Yes		
326.666+0.711	236.07	−54.00	Yes		
326.667+0.878	235.90	−53.86	Yes		
326.668+0.035	236.78	−54.53	Yes		
326.673+0.068	236.75	−54.50	Yes		
326.673+0.300	236.51	−54.32	Yes		
326.677+0.892	235.90	−53.85	Yes		
326.686−0.321	237.19	−54.80			No distinct core
326.699+0.869	235.95	−53.85	No	No	Confused at 500 μm
326.701−0.194	237.07	−54.69			No distinct core
326.704+0.741	236.09	−53.95	No	Yes	
326.706+0.347	236.50	−54.26			No distinct core
326.706+0.875	235.95	−53.84			No distinct core
326.718−0.127	237.02	−54.63	Yes		
326.720+0.032	236.86	−54.50	Yes		
326.724+0.337	236.54	−54.26	Yes		
326.735−0.093	237.01	−54.59	Yes		
326.745−0.147	237.08	−54.63	Yes		
326.750+0.133	236.79	−54.40			No distinct core
326.758+0.213	236.72	−54.33	Yes		
326.759−0.100	237.05	−54.58	Yes		
326.760−0.169	237.13	−54.63	Yes		
326.763+0.864	236.04	−53.82	Yes		
326.783−0.707	237.74	−55.04	Yes		
326.786−0.757	237.80	−55.08	No	Yes	
326.787−0.357	237.37	−54.76	Yes		
326.787−0.399	237.41	−54.80	Yes		
326.795−0.045	237.04	−54.51			No distinct core
326.811+0.511	236.47	−54.07	Yes		
326.811+0.656	236.32	−53.95	No	No	
326.812+0.425	236.56	−54.13	Yes		
326.815−0.772	237.86	−55.07	Yes		
326.824+0.466	236.54	−54.09	Yes		
326.826−0.315	237.37	−54.71	Yes		
326.826−0.753	237.85	−55.05			No distinct core
326.826+0.510	236.49	−54.06			No distinct core
326.828+0.072	236.96	−54.40	No	Yes	
326.831+0.549	236.46	−54.02			Stripy at 250 μm
326.834+0.582	236.43	−54.00			Stripy at 250 μm
326.835−0.069	237.12	−54.51	Yes		
326.836+0.068	236.97	−54.40			No distinct core
326.850+0.641	236.39	−53.94	Yes		
326.851+0.521	236.52	−54.03	No	No	Confused at 500 μm
326.857−0.311	237.41	−54.68	Yes		
326.857+0.496	236.55	−54.05	Yes		
326.870+0.071	237.02	−54.38	Yes		
326.872+0.410	236.66	−54.11	No	No	Confused at 500 μm

continued on next page

IRDC Name	Right Ascension 2000.0 (°)	Declination 2000.0 (°)	8 μm source?	24 μm source?	Additional comments
326.875+0.704	236.36	−53.87	No	No	Confused at 500 μm
326.876+0.639	236.43	−53.93			No distinct core
326.877−0.214	237.33	−54.60	Yes		
326.884+0.448	236.64	−54.07	Yes		
326.885+0.142	236.96	−54.31			No distinct core
326.886+0.307	236.79	−54.18	Yes		
326.889+0.294	236.81	−54.19	No	Yes	
326.890−0.350	237.50	−54.69	Yes		
326.898+0.155	236.96	−54.29	Yes		
326.900+0.568	236.53	−53.97			Stripy at 250 μm
326.902+0.839	236.25	−53.75	No	No	Confused at 160 μm
326.908+0.457	236.66	−54.05	Yes		
326.910+0.561	236.55	−53.97			Stripy at 250 μm
326.911+0.442	236.68	−54.06	No	No	Confused at 500 μm
326.917−0.038	237.20	−54.43	No	Yes	
326.923+0.452	236.68	−54.04	No	No	Confused at 500 μm
326.924+0.716	236.41	−53.84	Yes		
326.926+0.736	236.39	−53.82	No	No	Confused at 500 μm
326.928+0.427	236.72	−54.06			No distinct core
326.929+0.538	236.60	−53.97	Yes		
326.938+0.561	236.59	−53.95			Stripy at 250 μm
326.944+0.350	236.82	−54.11			No distinct core
326.950−0.164	237.38	−54.51	Yes		
326.951+0.325	236.86	−54.13			No distinct core
326.952−0.003	237.21	−54.38	Yes		
326.956−0.007	237.22	−54.38	Yes		
326.956+0.497	236.68	−53.99	Yes		
326.956+0.517	236.66	−53.97	Yes		
326.959+0.463	236.72	−54.01	No	No	Confused at 500 μm
326.962+0.451	236.74	−54.02	Yes		
326.970−0.033	237.26	−54.40	Yes		
326.992+0.007	237.25	−54.35			No distinct core
326.995−0.183	237.46	−54.50	Yes		
327.002−0.174	237.46	−54.49	No	Yes	
327.004−0.079	237.36	−54.41	Yes		
327.010−0.032	237.32	−54.37	No	Yes	
327.019+0.008	237.29	−54.33	Yes		
327.021−0.162	237.47	−54.47	No	Yes	
327.023+0.477	236.79	−53.96	Yes		
327.025−0.045	237.35	−54.37	No	Yes	
327.027−0.296	237.62	−54.57	No	Yes	
327.034−0.110	237.43	−54.42	No	Yes	
327.043−0.290	237.64	−54.55	No	Yes	
327.044+0.019	237.31	−54.31	Yes		
327.049−0.302	237.66	−54.56	No	Yes	
327.069−0.288	237.67	−54.53	Yes		
327.074−0.012	237.38	−54.32	No	Yes	
327.076−0.104	237.48	−54.39	Yes		
327.086+0.007	237.38	−54.29	No	Yes	
327.090−0.250	237.66	−54.49	Yes		
327.093−0.350	237.77	−54.57	Yes		
327.098+0.234	237.15	−54.11	Yes		
327.112−0.291	237.73	−54.51	Yes		
327.123+0.723	236.67	−53.71	No	No	Confused at 500 μm
327.129−0.461	237.94	−54.63	No	Yes	
327.143−0.335	237.82	−54.52	Yes		
327.144−0.303	237.79	−54.50	Yes		
327.162−0.337	237.85	−54.51	Yes		
327.167−0.300	237.81	−54.48	Yes		

continued on next page

IRDC Name	Right Ascension 2000.0 (°)	Declination 2000.0 (°)	8 μm source?	24 μm source?	Additional comments
327.224+0.225	237.33	−54.04			No distinct core
327.237+0.231	237.34	−54.02	No	Yes	
327.238+0.241	237.33	−54.01			No distinct core
327.251−0.134	237.75	−54.30	Yes		
327.252−0.093	237.71	−54.27			No distinct core
327.277+0.224	237.40	−54.00	Yes		
327.391−0.387	238.21	−54.41	No	No	Confused at 500 μm
327.402−0.416	238.25	−54.42	No	Yes	
327.429−0.397	238.27	−54.39	Yes		
327.457−0.694	238.63	−54.60	Yes		
327.485+0.761	237.11	−53.45	Yes		
327.486−0.694	238.67	−54.58	Yes		
327.491−0.311	238.26	−54.29	Yes		
327.535−0.534	238.56	−54.43	No	Yes	
327.572+0.326	237.68	−53.74	Yes		
327.610+0.802	237.23	−53.34	Yes		
327.653−0.605	238.79	−54.41			No distinct core
327.659+0.609	237.50	−53.46			No distinct core
327.676−0.566	238.78	−54.36	Yes		
327.683−0.543	238.76	−54.34	Yes		
327.695−0.552	238.79	−54.34			No distinct core
327.723−0.535	238.81	−54.31	Yes		
327.725+0.894	237.28	−53.20	No	No	Confused at 500 μm
327.727−0.566	238.85	−54.33	Yes		
327.729−0.051	238.29	−53.93			No distinct core
327.746+0.925	237.28	−53.16	No	Yes	
327.753−0.090	238.37	−53.95	Yes		
327.763−0.513	238.84	−54.27			No distinct core
327.765−0.490	238.82	−54.25	No	Yes	
327.778−0.091	238.40	−53.93	Yes		
327.787−0.491	238.85	−54.24	Yes		
327.795−0.466	238.83	−54.21			No distinct core
327.804+0.064	238.26	−53.80	Yes		
327.808+0.495	237.81	−53.46	Yes		
327.811−0.288	238.66	−54.06	No	Yes	
327.815−0.560	238.96	−54.27	Yes		
327.815+0.488	237.83	−53.46	Yes		
327.816−0.451	238.84	−54.19	Yes		
327.848−0.479	238.91	−54.19			No distinct core
327.852+0.503	237.86	−53.43	Yes		
327.863+0.470	237.91	−53.44	Yes		
327.880−0.461	238.94	−54.15	Yes		
327.887−0.474	238.96	−54.16			No distinct core
327.893+0.435	237.99	−53.45	No	Yes	
327.914−0.611	239.14	−54.25	Yes		
327.917−0.397	238.91	−54.08			No distinct core
327.923+0.566	237.89	−53.33			No distinct core
327.924−0.536	239.07	−54.18			No distinct core
327.929+0.430	238.04	−53.43	No	Yes	
327.936+0.511	237.96	−53.37	No	No	Confused at 500 μm
327.937−0.538	239.09	−54.18			No distinct core
327.950−0.723	239.31	−54.31	Yes		
327.952+0.520	237.97	−53.35	Yes		
327.964+0.388	238.13	−53.44	Yes		
327.974+0.371	238.16	−53.45	Yes		
327.980−0.490	239.10	−54.11	Yes		
327.988−0.711	239.35	−54.27	No	Yes	
327.990+0.506	238.04	−53.34	Yes		
328.004−0.509	239.15	−54.11			No distinct core

continued on next page

IRDC Name	Right Ascension 2000.0 (°)	Declination 2000.0 (°)	8 μm source?	24 μm source?	Additional comments
328.007+0.416	238.15	−53.40	Yes		
328.022+0.382	238.21	−53.41			No distinct core
328.035+0.615	237.98	−53.22	Yes		
328.036+0.395	238.21	−53.39	Yes		
328.044−0.391	239.07	−53.99	No	Yes	
328.050−0.538	239.24	−54.10	Yes		
328.054−0.026	238.69	−53.71	Yes		
328.057−0.293	238.98	−53.91			No distinct core
328.061−0.278	238.97	−53.90			No distinct core
328.068−0.284	238.99	−53.90	No	Yes	
328.068+0.513	238.13	−53.28	Yes		
328.073−0.128	238.82	−53.77			No distinct core
328.077+0.528	238.13	−53.26			No distinct core
328.086−0.102	238.81	−53.75			No distinct core
328.088−0.321	239.05	−53.91	Yes		
328.094+0.567	238.11	−53.22			No distinct core
328.100−0.542	239.31	−54.07	No	Yes	
328.101+0.626	238.05	−53.17	Yes		
328.102+0.368	238.33	−53.37	Yes		
328.103−0.445	239.21	−54.00	Yes		
328.103+0.602	238.08	−53.19	No	Yes	
328.108−0.175	238.92	−53.79			No distinct core
328.108−0.383	239.15	−53.95	No	Yes	
328.119+0.358	238.36	−53.37	No	Yes	
328.163−0.282	239.11	−53.83	Yes		
328.167+0.021	238.78	−53.60			No distinct core
328.175+0.310	238.48	−53.37	Yes		
328.176−0.671	239.55	−54.12	Yes		
328.178+0.285	238.51	−53.39	No	Yes	
328.196−0.672	239.58	−54.11			Stripy at 250 μm
328.220−0.392	239.30	−53.88	Yes		
328.220+0.094	238.77	−53.51	Yes		
328.227−0.378	239.29	−53.87			No distinct core
328.232−0.367	239.29	−53.86	Yes		
328.251−0.301	239.24	−53.79			No distinct core
328.255−0.412	239.37	−53.87	Yes		
328.258−0.255	239.20	−53.75	Yes		
328.264−0.302	239.26	−53.78	Yes		
328.273−0.193	239.15	−53.70	Yes		
328.274+0.596	238.31	−53.09			No distinct core
328.282−0.046	239.01	−53.58	Yes		
328.303−0.106	239.10	−53.61	No	Yes	
328.303−0.302	239.31	−53.76	No	Yes	
328.304−0.012	239.00	−53.54	Yes		
328.309+0.237	238.74	−53.34			No distinct core
328.311−0.549	239.59	−53.94	Yes		
328.320−0.521	239.57	−53.92			No distinct core
328.348−0.246	239.31	−53.69	No	Yes	
328.386−0.308	239.43	−53.71	Yes		
328.397−0.336	239.47	−53.72	Yes		
328.400−0.495	239.65	−53.84			Stripy at 250 μm
328.406−0.085	239.21	−53.53	No	Yes	
328.409−0.109	239.24	−53.54	Yes		
328.424+0.070	239.06	−53.40	Yes		
328.432−0.522	239.72	−53.84	No	No	
328.433+0.594	238.51	−52.99	Yes		
328.514+0.276	238.96	−53.18			No distinct core
328.584+0.645	238.65	−52.85	No	No	Confused at 500 μm
328.624+0.274	239.10	−53.11	Yes		

continued on next page

IRDC Name	Right Ascension 2000.0 (°)	Declination 2000.0 (°)	8 μm source?	24 μm source?	Additional comments
328.641−0.303	239.75	−53.54			No distinct core
328.657−0.422	239.90	−53.62	Yes		
328.665+0.502	238.91	−52.91	Yes		
328.684+0.018	239.45	−53.27	Yes		
328.690−0.310	239.82	−53.51	Yes		
328.693+0.255	239.21	−53.08			No distinct core
328.741+0.614	238.89	−52.78	No	Yes	
328.755+0.606	238.91	−52.77	No	Yes	
328.762+0.354	239.19	−52.96	Yes		
328.765+0.716	238.81	−52.68	Yes		
328.768+0.664	238.87	−52.72	Yes		
328.771−0.570	240.21	−53.66			Stripy at 250 μm
328.816+0.745	238.84	−52.63			Stripy at 250 μm
328.822+0.468	239.15	−52.84			No distinct core
328.822+0.753	238.84	−52.62			Stripy at 250 μm
328.834+0.457	239.17	−52.84			No distinct core
328.854+0.752	238.88	−52.60			Stripy at 250 μm
328.859+0.277	239.40	−52.96	Yes		
328.865+0.752	238.90	−52.59			Stripy at 250 μm
328.869+0.257	239.43	−52.97	Yes		
328.899+0.750	238.94	−52.57	Yes		
328.904−0.101	239.86	−53.22			No distinct core
328.913−0.099	239.87	−53.21			No distinct core
328.923+0.284	239.47	−52.91	Yes		
328.947+0.369	239.41	−52.83	No	Yes	
328.951+0.816	238.94	−52.49	No	No	Confused at 500 μm
328.992+0.786	239.02	−52.48	No	No	Confused at 500 μm
329.021−0.166	240.08	−53.19			No distinct core
329.028−0.202	240.13	−53.21	Yes		
329.039−0.119	240.05	−53.14	Yes		
329.039−0.140	240.08	−53.16	No	Yes	
329.042−0.177	240.12	−53.18			No distinct core
329.042−0.281	240.23	−53.26	Yes		
329.058−0.289	240.26	−53.26	Yes		
329.067−0.112	240.08	−53.12			No distinct core
329.077+0.415	239.52	−52.71	No	Yes	
329.088−0.399	240.42	−53.32	Yes		
329.101−0.394	240.43	−53.31	Yes		
329.114−0.379	240.43	−53.29	No	No	Confused at 500 μm
329.169−0.745	240.91	−53.53	Yes		
329.178−0.602	240.76	−53.42	Yes		
329.179+0.446	239.62	−52.62	Yes		
329.201+0.559	239.53	−52.52	Yes		
329.208−0.742	240.95	−53.50			No distinct core
329.213−0.757	240.97	−53.51	Yes		
329.227+0.482	239.64	−52.56	Yes		
329.247−0.233	240.44	−53.09	No	Yes	
329.251−0.267	240.48	−53.12	No	No	Confused at 500 μm
329.265−0.339	240.58	−53.16			Stripy at 250 μm
329.276−0.258	240.50	−53.09	Yes		
329.278−0.341	240.60	−53.15			Stripy at 250 μm
329.313−0.302	240.60	−53.10	Yes		
329.374−0.284	240.65	−53.05	Yes		
329.389−0.659	241.09	−53.32	Yes		
329.403−0.736A	241.19	−53.37	Yes		
329.403−0.736B	241.19	−53.37	No	No	
329.413−0.226	240.64	−52.98	Yes		
329.424+0.475	239.89	−52.44	No	Yes	
329.437+0.853	239.51	−52.14	Yes		

continued on next page

IRDC Name	Right Ascension 2000.0 (°)	Declination 2000.0 (°)	8 μm source?	24 μm source?	Additional comments
329.441+0.518	239.87	−52.40	Yes		
329.444−0.765	241.27	−53.36	Yes		
329.463−0.770	241.30	−53.35	Yes		
329.463+0.517	239.90	−52.38	Yes		
329.489+0.404	240.05	−52.45	Yes		
329.494+0.106	240.38	−52.67	Yes		
329.557−0.362	240.97	−52.99	Yes		
329.568−0.354	240.97	−52.97	Yes		
329.568−0.392	241.01	−53.00	Yes		
329.589+0.045	240.56	−52.66	Yes		
329.621−0.407	241.10	−52.98			No distinct core
329.627+0.855	239.74	−52.02	No	No	Confused at 500 μm
329.633−0.387	241.09	−52.95	No	Yes	
329.638+0.836	239.78	−52.03	Yes		
329.642+0.908	239.70	−51.97	Yes		
329.648+0.857	239.76	−52.00	Yes		
329.648+0.957	239.66	−51.93	Yes		
329.652+0.073	240.61	−52.59	No	Yes	
329.655+0.852	239.78	−52.00			No distinct core
329.684+0.819	239.85	−52.01	Yes		
329.684+0.875	239.79	−51.97	No	No	Confused at 500 μm
329.691−0.353	241.12	−52.89			No distinct core
329.726+0.848	239.87	−51.96			No distinct core
329.745−0.038	240.85	−52.62	Yes		
329.748+0.855	239.89	−51.94	No	No	Confused at 500 μm
329.749+0.868	239.88	−51.93	No	Yes	
329.863+0.456	240.46	−52.17	Yes		
329.875+0.121	240.83	−52.41	Yes		
329.902+0.969	239.96	−51.75			No distinct core
329.904+0.417	240.55	−52.17	Yes		
329.938−0.113	241.16	−52.55	Yes		
329.989−0.396	241.54	−52.72	Yes		

APPENDIX B: TESTING THE CATALOGUE COMPLETENESS

In the main body of this paper, we search for IRDCs within the area $l = 300 - 330\,^\circ$, $|b| < 1\,^\circ$ using the catalogue of PF09. They used *Spitzer* 8-μm data to identify 11303 candidate IRDCs in the Galactic Plane. 3171 of these lie in our search area. To ascertain how many IRDCs may have been missed due to sensitivity limits we modelled several IRDCs and placed them in the Hi-GAL data in regions with differing backgrounds. The modelled IRDCs were observed in the same manner as the original candidates. The dimensions and flux levels of the smallest visible IRDC were determined.

To model the IRDCs we used PHAETHON (Stamatellos & Whitworth 2003, 2005; Stamatellos et al. 2010). PHAETHON is a 3D Monte Carlo radiative transfer code and has been used previously to model IRDCs (Stamatellos et al. 2010; Wilcock et al. 2011). The code uses luminosity packets to represent the ambient radiation field in the system. These packets are injected into the system where they interact (are absorbed, re-emitted or scattered) with it stochastically. The ambient radiation field is taken to be a multiple of a modified version of the Black (1994) interstellar radiation field (ISRF), which gives a good approximation to the radiation field in the solar neighbourhood. The input variables of the code are the density profile, the strength of the ambient radiation field, the dust properties of the system, the size of the core and its geometry.

IRDCs were created with three different radii (0.2, 0.4 and 0.7 pc) and two different peak column densities (the detection threshold of PF09, $2{\times}10^{22}$ cm^{-2}, and $4{\times}10^{22}$ cm^{-2}). Using the mean parameters of IRDCs modelled by Wilcock et al. (2012), we place our model IRDCS at a distance of 3.1 kpc and use a surrounding ISRF of 3.2 times the Black (1994) radiation field. As most IRDCs do not appear spherical, they were modelled with a flattened geometry which has a density profile given by:

$$n\,(r,\theta) = n_0\,(\mathrm{H_2})\,\frac{1 + A\left(\frac{r}{R_0}\right)^2[\sin(\theta)]^2}{\left[1 + \left(\frac{r}{R_0}\right)^2\right]^2}, \tag{B1}$$

where r is the radial distance, θ is the polar angle and R_0 is the flattening radius (i.e. the radial distance for which the central density is approximately constant). $n_0(\mathrm{H_2})$ is the central density, which is controlled as an input variable. A is a factor that controls the equatorial to polar optical depth ratio and determines how flattened the core is. This was set at 2.5 and corresponds to an aspect ratio of $\sim 1:7$. R_0 was one tenth of the maximum radius. The dust opacity at 500 μm used was 0.03 cm^2 g^{-1} (Ossenkopf & Henning 1994).

Each of the six IRDCs was convolved with the telscope beam at each wavelength and placed into the Hi-GAL data in four positions. The locations selected were typical areas within the Hi-GAL field that did not contain any candidate IRDCs and were chosen to cover a range of different background levels. These were: Position A ($l = 327.829\,^\circ$, $b = +0.17\,^\circ$), a confused region near the centre of the Galactic Plane which has the highest background level at 2600 MJy sr^{-1} at 250 μm; Position B ($l = 328.427\,^\circ$, $b = +0.04\,^\circ$), an unconfused area, also near the centre of the Galactic Plane, with a background of 1300 MJy sr^{-1} at 250 μm; Position C ($l = 328.141\,^\circ$, $b = -0.89\,^\circ$), a confused area near the edge of the Hi-GAL data with a background level of 450 MJy sr^{-1} at 250 μm; and Position D ($l = 327.973\,^\circ$, $b = -0.99\,^\circ$), an unconfused area with the lowest background at 65MJy sr^{-1} at 250 μm. We define a confused region as one with many nearby sources. Figures B1–B4 shown these four regions as they appear in the observations.

Synthetic observations were created of the model IRDCS in each position at *Spitzer* 8 μm and *Herschel* 70, 160, 250, 350 and 500 μm. As with the original candidates, if the IRDC was seen in emission at the three longest wavelengths it was then classed as *Spitzer*-dark and *Herschel*-bright and thus a genuine IRDC. If there was no clear emission then it was classed as *Spitzer*-dark and *Herschel*-dark and so dismissed. As PHAETHON only models the emission of the IRDC, the 8 and 70 μm maps with the added IRDCs appears no different from the original data and so are not necessarily Spitzer-dark.

The smallest modelled IRDC (0.2 pc, $2{\times}10^{22}$ cm^{-2}) can clearly be seen in emission in Positions B, C and D but not in Position A. This can be seen in Figures B5–B8. A small amount of emission can be seen from the 0.2 pc IRDC with a peak column density of $4{\times}10^{22}$ cm^{-2} and the 0.4 pc, $2{\times}10^{22}$ cm^{-2} IRDC (Figures B9 and B10, respectively) in Position A, although it can not be stated with absolute certainty that these objects would have been classed as *Herschel*-bright. The smallest IRDC that can clearly be seen in emission at the highest background levels is 0.4 pc in radius with a peak column density of $4{\times}10^{22}$ cm^{-2}, shown in Figure B11. We therefore conclude that any IRDC whose major axis is $\leqslant 26''$(corresponding to 0.4 pc at a distance of 3.1 kpc) with a peak column density less than $4{\times}10^{22}$ cm^{-2} in an area where the background level is greater than 1300 MJy sr^{-1} at 250 μm may not be found to be *Herschel*-bright, regardless of whether it is a genuine IRDC or not (although some were). A quantitative analysis of *Herschel*-bright IRDC detections as a function of their physical parameters will be addressed in Lenfestey et al. (2012).

We then attempted to estimate what percentage of the PF09 catalogue falls below our sensitivity limits. We focussed on a 2 degree-square region centred on $l = 327\,^\circ$, $b = 0\,^\circ$. This area was chosen as it is typical of the $l = 300 - 330\,^\circ$ region and contains many candidate IRDCs.

The background levels ranged from approximately 390 to 2900 MJy sr^{-1} (equivalent to Positions C and A respectively), with an average of 1400 MJy sr^{-1} (equivalent to Position B). The background levels were defined using an aperture close to the position of each candidate IRDC. Using axis size and peak opacities from PF09 we isolated those candidates that fall below our completeness criteria. The column density of each was calculated using:

$$N_{H_2} = \tau_{8\,\mu m} \times 3\,[\pm 1] \times 10^{22}\ \mathrm{cm^{-2}}, \tag{B2}$$

(PF09), where N_{H_2} is the peak column density of the IRDC and $\tau_{8\,\mu m}$ is the peak 8 μm opacity taken from PF09.

This region contains 690 IRDC candidates. 141 of these are *Herschel*-dark with a radius less than $26''$, a peak column density lower than $4{\times}10^{22}$ cm^{-2} and a background level above 1300 MJy sr^{-1}. For these 141 objects we can not state their true status. Therefore, the unknown objects comprise 141/690, or approximately 20%, of the PF09 IRDC candidates in the $2 \times 2\,^\circ$ area.

We therefore surmise that, if this pattern is typical of the whole Galactic Plane, then ∼20% are unlikely to be seen in emission by *Herschel* regardless of their true status, ∼40% of the PF09 candidate IRDCS are *Herschel*-bright, ∼40% are *Herschel*-dark.

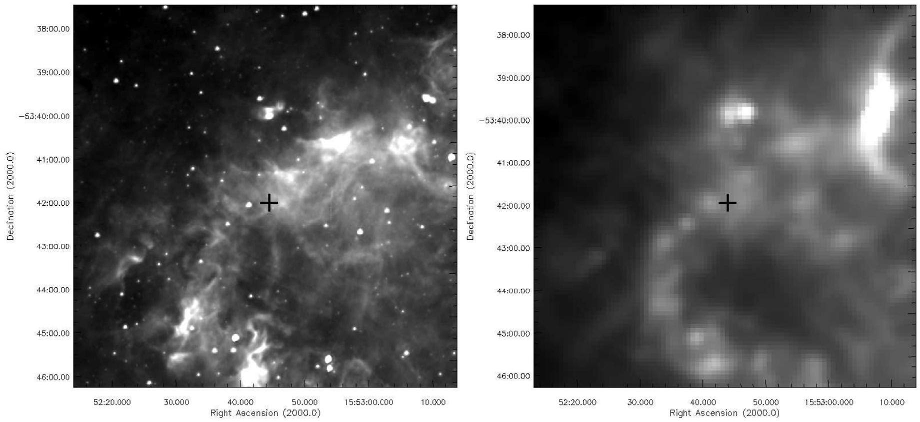

Figure B1. Position A, shown without the addition of any modelled IRDCs, at 8 μm (left) and 250 μm (right). A cross marks the point where the IRDCs are added.

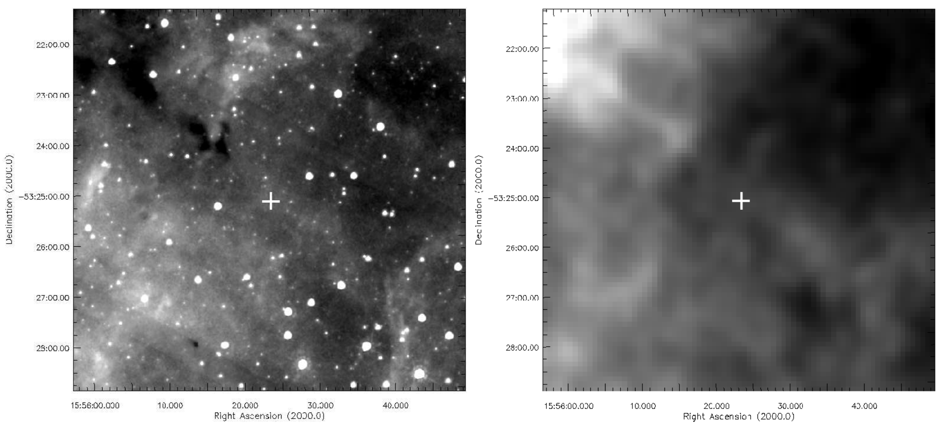

Figure B2. Position B, shown without the addition of any modelled IRDCs, at 8 μm (left) and 250 μm (right). A cross marks the point where the IRDCs are added.

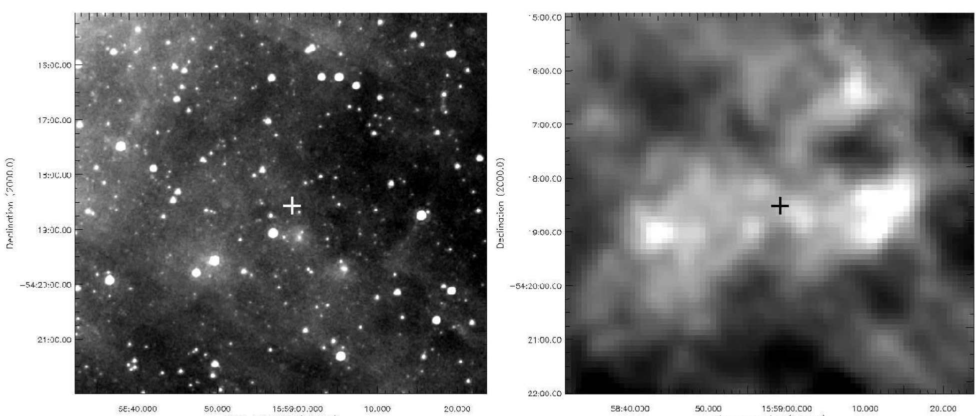

Figure B3. Position C, shown without the addition of any modelled IRDCs, at 8 μm (left) and 250 μm (right). A cross marks the point where the IRDCs are added.

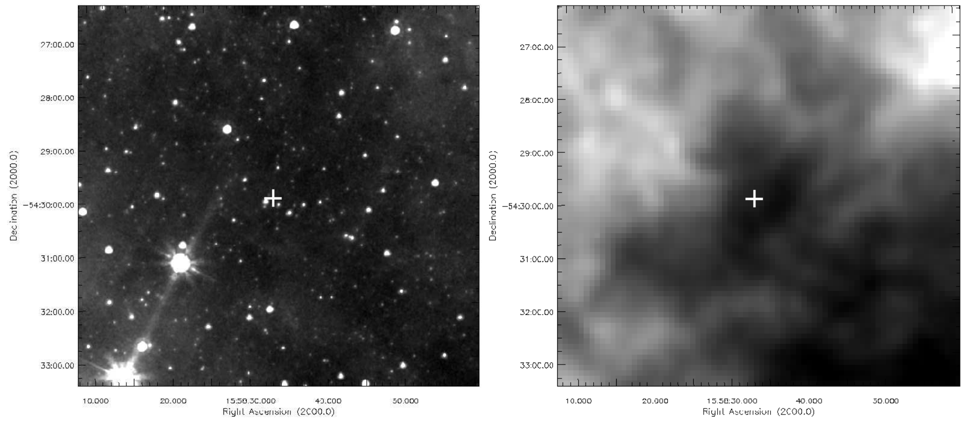

Figure B4. Position D, shown without the addition of any modelled IRDCs, at 8 μm (left) and 250 μm (right). A cross marks the point where the IRDCs are added.

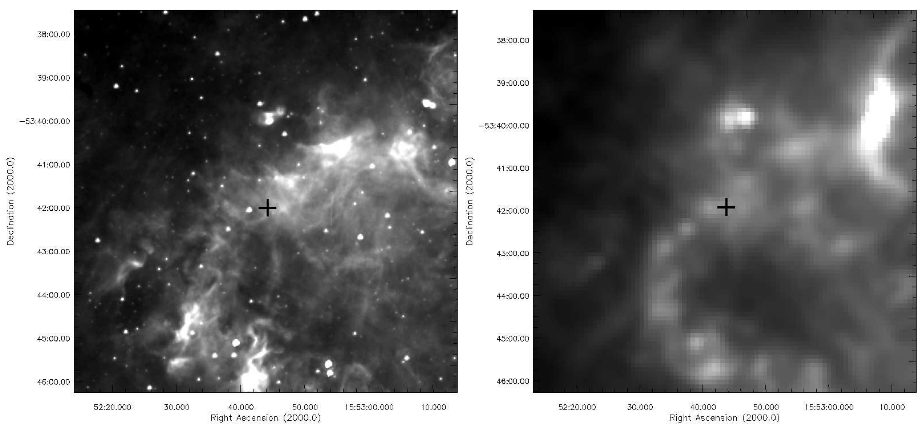

Figure B5. A core with radius 0.2 pc and a peak column density of $2{\times}10^{22}$ cm^{-2} placed in Position A. The IRDC is shown at 8 μm (left) and 250 μm (right). A cross marks the position of the IRDC.

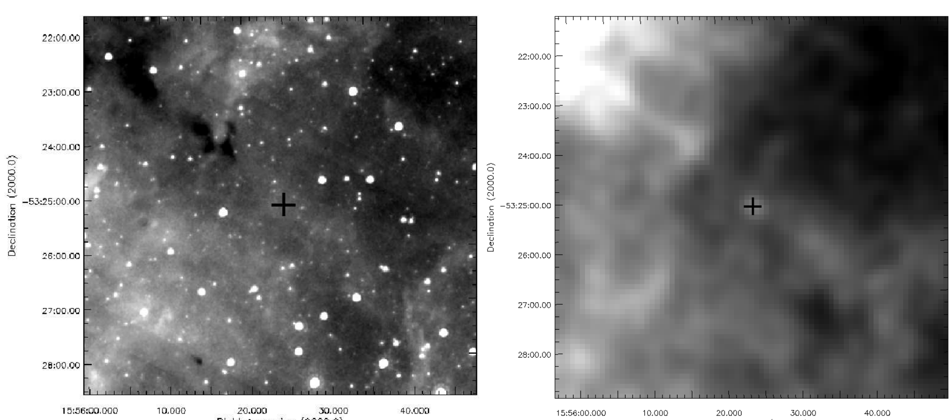

Figure B6. A core with radius 0.2 pc and a peak column density of $2{\times}10^{22}$ cm^{-2} placed in Position B. The IRDC is shown at 8 μm (left) and 250 μm (right). A cross marks the position of the IRDC.

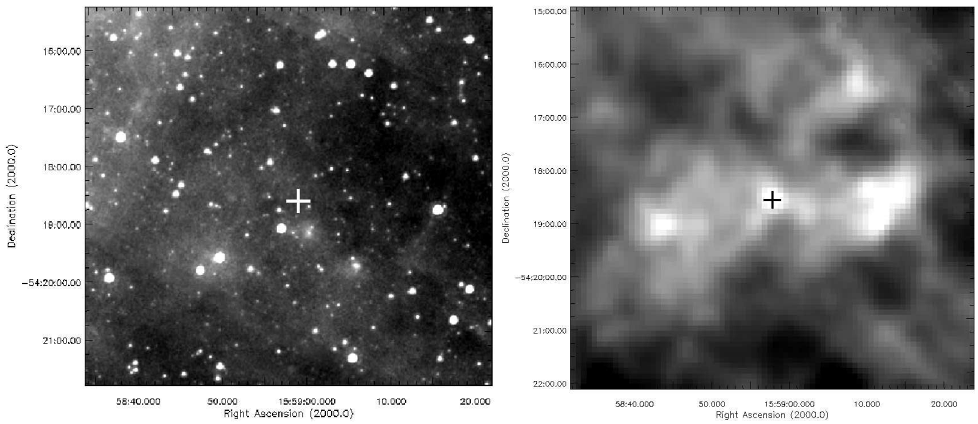

Figure B7. A core with radius 0.2 pc and a peak column density of $2{\times}10^{22}$ cm^{-2} placed in Position C. The IRDC is shown at 8 μm (left) and 250 μm (right). A cross marks the position of the IRDC.

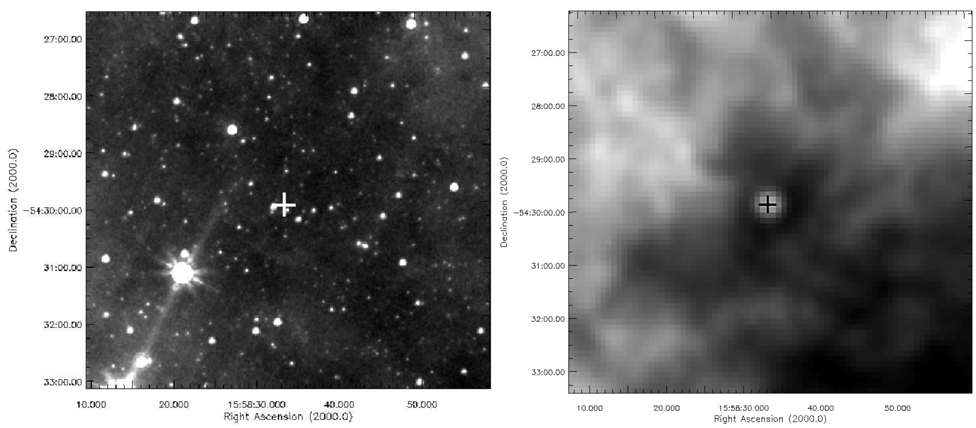

Figure B8. A core with radius 0.2 pc and a peak column density of $2{\times}10^{22}$ cm^{-2} placed in Position D. The IRDC is shown at 8 μm (left) and 250 μm (right). A cross marks the position of the IRDC.

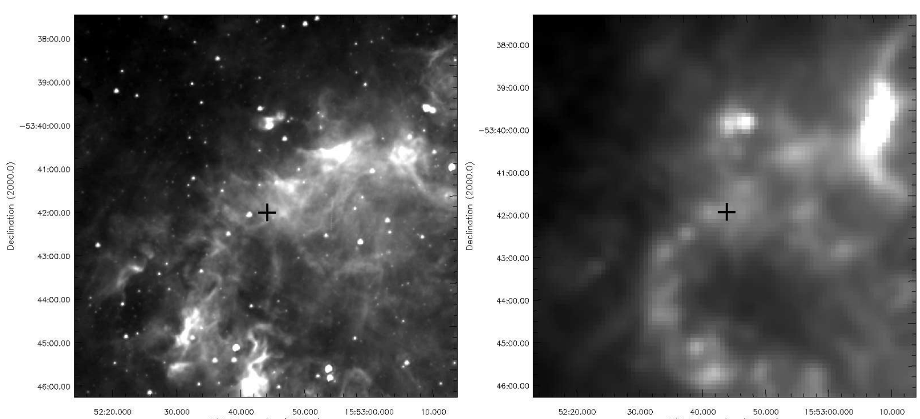

Figure B9. A core with radius 0.2 pc and a peak column density of $4{\times}10^{22}$ cm^{-2} placed in Position A. The IRDC is shown at 8 μm (left) and 250 μm (right). A cross marks the position of the IRDC.

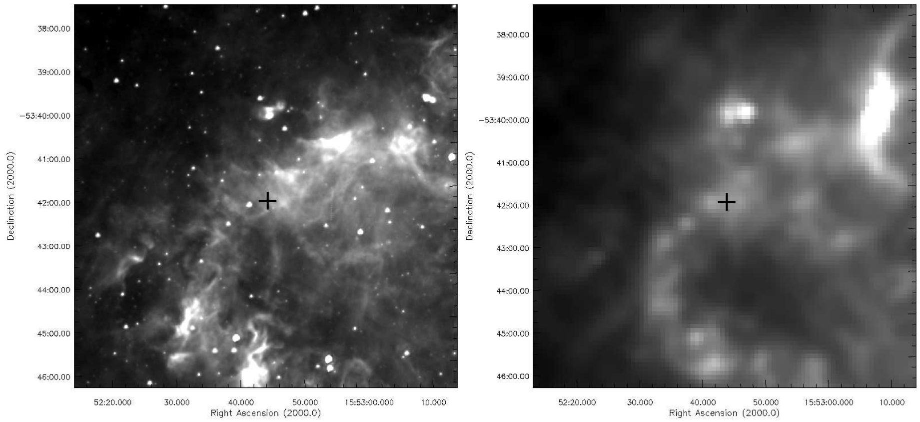

Figure B10. A core with radius 0.4 pc and a peak column density of $2{\times}10^{22}$ cm^{-2} placed in Position A. The IRDC is shown at 8 μm (left) and 250 μm (right). A cross marks the position of the IRDC.

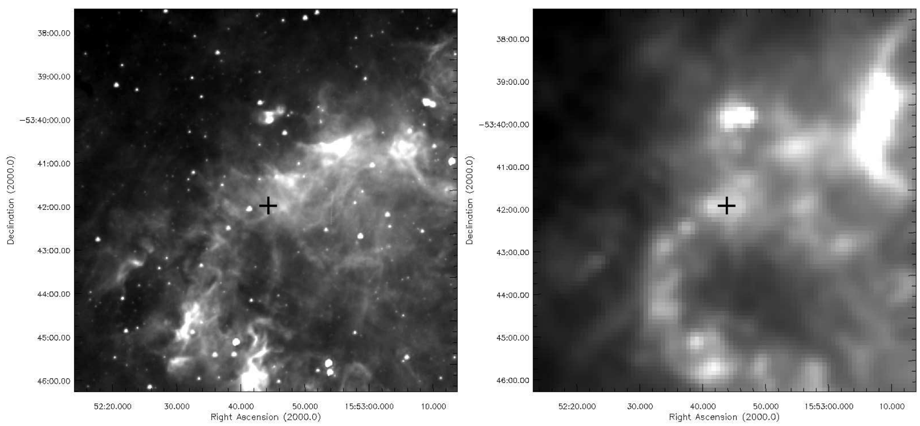

Figure B11. A core with radius 0.4 pc and a peak column density of $4{\times}10^{22}$ cm^{-2} placed in Position A. The IRDC is shown at 8 μm (left) and 250 μm (right). A cross marks the position of the IRDC.